STATISTICAL SHAPE MODELING TO QUANTIFY VARIATION IN THE PROXIMAL HUMERAL ANATOMY

_____

A Thesis

Presented to

the Faculty of the Daniel Felix Ritchie School of Engineering and Computer Science

University of Denver

_____

In Partial Fulfillment

of the Requirements for the Degree

Master of Science

_____

by

Paul B. Sade Sr.

June 2017

Advisor: Dr. Peter Laz

Author: Paul B. Sade Sr.
Title: STATISTICAL SHAPE MODELING TO QUANTIFY VARIATION IN THE PROXIMAL HUMERAL ANATOMY
Advisor: Dr. Peter Laz
Degree Date: June 2017

ABSTRACT

The fit of the humeral prosthesis to the intramedullary canal and the replication of the anatomic humeral head center are important factors in Total Shoulder Arthroplasty (TSA). The objective of this thesis was to develop a Statistical Shape Model (SSM) of the cortical and cancellous bone regions of the proximal humerus, and to assess potential shape differences with gender and ethnicity, with a goal of informing implant design. An SSM was used and Principal Component Analysis (PCA) was applied to data that represented both the cancellous and cortical humeral bone of 63 healthy subjects and cadavers. Anatomical measurements and PC scores were analyzed by gender and ethnicity. Scaling accounted for 75% of the variation in the training set. Differences between males and females were primarily in size. Ethnicity differences were observed in the relationship between medial and posterior offset. Differences in ethnicity and/or gender were observed in the relationship between posterior offset and the head inclination angle. These are differences that should be considered when designing implants for a global population or subpopulation.

ACKNOWLEDGEMENTS

I'd like to first acknowledge my advisor, Dr. Peter Laz, and thank him for his support, guidance, and nudging. I greatly appreciate his experience, responsiveness, patience, and tact.

In the computational biomechanics lab, Irene Sintini has been an invaluable resource and extremely competent. Her patience and responsiveness to my many stupid questions is greatly appreciated.

Justin Hollenbeck, Will Burton, and Lowell Smoger, were very gracious lab members and helped get me off to a good start on my research and keep me going in the right direction. I also want to thank Dr. Paul Rullkoetter for his patience during the many courses he taught and his guidance when beginning the program. Thanks to Dr. Rachel Epstein for graciously agreeing to be the external chairperson on short notice.

Appreciation goes to my co-workers Jason Chavarria, Anthony Webb, and Dan Huff for product knowledge, advice, Matlab tips, and encouragement.

And I certainly would not have made it through the program if it weren't for my fellow students, friends, and partners in the grind, Rod Satterthwaite and Ryan Keefer. Our many hours together studying and not studying will long be remembered.

Lastly, I would to thank my wife, Michele, for her steady and unending support for not only the past 4 ½ years of this program, but for the past 26.

TABLE OF CONTENTS

List of Figures vi

List of Tables viii

Chapter 1: Introduction 1
1.1 Motivation and Project Objectives 1
1.2 Organization 2

Chapter 2: Review of Literature 4
2.1 Anatomy of the Shoulder 4
2.2 Shoulder Conditions 6
2.2.1 Arthritis 8
2.2.2 Other Shoulder Conditions 8
2.3 Shoulder Treatments 9
2.3.1 RICE 9
2.3.2 Medication 10
2.3.3 Physical Therapy 10
2.3.4 Surgery 10
2.3.4.1 Arthroscopic Surgery 11
2.3.4.2 Partial and Total Shoulder Replacement 11
2.3.4.3 Shoulder Resurfacing 14
2.3.4.4 Cuff-Tear Arthropathy Repair 16
2.3.4.5 Reverse Shoulder Replacement 16
2.3.4.6 Fracture Surgery 18
2.4 Complications with Shoulder Arthroplasty 20
2.5 Anatomical Considerations When Designing A Stem Prosthesis 23
2.6 Statistical Shape Modeling 25

Chapter 3: Methods 29
3.1 Population Selection: Training Set 29
3.2 Data Processing 30
3.2.1 Segmentation 30
3.2.2 Pre-processing 32
3.2.3 Processing 32

Chapter 4: Results 36
4.1 Modes of Variation 36
4.2 Leave-one-out Analysis 37
4.3 PC Correlations 38
4.4 Anatomical Measurement Correlations 40

Chapter 5: Discussion 49
5.1 Significance 49
5.2 Limitations 53
5.3 Conclusion 54

References 56

Appendix A: Training Set 61

Appendix B: Description of Anatomical Measurements 63

LIST OF FIGURES

Number *Page*

2.1 Bones of the shoulder 5
2.2 Glenohumeral joint and acromioclavicular joint 5
2.3 Soft tissues of the shoulder. 6
2.4 Example of an arthritic shoulder 7
2.5 Example of a total shoulder replacement 12
2.6 Example of shoulder resurfacing 14
2.7 Example of cuff-tear arthropathy 16
2.8 Example of a reverse shoulder replacement 17
2.9 Example of a shoulder fracture 18
2.10 Anatomy of the proximal humerus 23

3.1 Example of a segmented proximal humerus 31
3.2 Trimming the humerus 32

4.1 Principal components - % of variation 36
4.2 Principal components showing mean +/- 2 standard deviations 37
4.3 Mode 1 vs. head radius 38
4.4 Mode 1 vs. articular surface thickness 38
4.5 Mode 1 vs. greater tuberosity offset 38
4.6 Mode 1 vs. canal diameter 38
4.7 Mode 3 vs. inclination 39
4.8 Mode 3 vs. neck angle 39
4.9 Mode 3 vs. medial offset 39
4.10 Mode 4 vs. canal diameter 40
4.11 Mode 4 vs. AP offset 40
4.12 head radius vs. articular surface thickness 41
4.13 head radius vs. greater tuberosity offset 41
4.14 head radius vs. canal diameter 41
4.15 neck angle vs. inclination 42
4.16 neck angle vs. medial offset 42
4.17 greater tuberosity offset vs. articular surface thickness 42
4.18 AP offset vs. inclination 42
4.19 medial offset vs. inclination 43
4.20 medial offset vs. AP offset 43
4.21 AP offset vs. inclination 45
4.22 medial offset vs. AP offset – Caucasians 46
4.23 medial offset vs. AP offset – Asians 46
4.24 medial offset vs. AP offset – males 47

4.25 medial offset vs. AP offset – females 47
4.26 medial offset vs. AP offset – Caucasian females 47
4.27 medial offset vs. AP offset – Asian females..... 47
4.28 medial offset vs. AP offset – Caucasian males..... 48
4.29 medial offset vs. AP offset – Asian males..... 48

5.1 Mode 3 captured changes in medial curve. 50
5.2 Medial offset vs. AP offset with implant offset ranges. 52

LIST OF TABLES

Number *Page*

2.1 Reasons for primary total shoulder replacement 14
2.2 Reasons for shoulder resurfacing 15
2.3 Causes of reverse shoulder replacement 18
2.4 Reasons for partial shoulder replacement 19
2.5 Reasons for revision shoulder surgery 21
2.6 Shoulder revision rates by brand of prosthesis 22

3.1 Subject age data 29
3.2 Caucasian subject data 30

4.1 Anatomical measurement correlations 40
4.2 Subgroup correlations for medial offset vs. inclination 44
4.3 Subgroup correlations for medial offset vs. neck angle 44
4.4 Subgroup correlations for AP offset vs. inclination 45
4.5 Subgroup correlations for medial offset vs. AP offset 46

5.1 RMS error results for SSM studies 49

CHAPTER 1: INTRODUCTION

1.1 Motivation and Project Objectives

Statistical shape models (SSM) have been used widely in a variety of fields to characterize variation within a data set and predict a new instance from, and among, the data set. In the field of orthopedic implant design, sizing for a broad population has historically been based on two-dimensional analysis from medical imaging (Hertel et al., 2002; Boileau and Walch, 1997; Humphrey et al., 2016).

While total shoulder arthroplasty (TSA) is an effective solution for many shoulder conditions, complications can arise from TSA. A percentage of these complications may result from improper sizing of the implant to the bone of the humerus. When using a shoulder prosthesis, replication of the anatomic humeral head center and the appropriate mating of a humeral stem in the intramedullary canal are important factors, both of which should be determined by the geometry of the native bone. Additionally, quality bone may need to be removed to accommodate an implant that doesn't properly match the patient anatomy. Better understanding of the differences in the geometry of the proximal humerus across a population could inform the design of future shoulder implants and surgical instruments. This in turn could drive better replication of the original anatomy for better

load transfer, and joint stability and mechanics, thereby leading to faster recoveries and better patient outcomes.

Using an SSM to create three-dimensional bone shapes for larger populations with a relatively small number of samples can be a cost effective method of ensuring the size extremes of the wider population are considered. Accordingly, the objective of this thesis was to develop a SSM of the cortical and cancellous bone regions of the proximal humerus, and to assess potential shape differences with gender and ethnicity, with the goal of informing humeral implant design and sizing.

1.2 Organization

The organization of this document is as follows:

Chapter 2 consists of literature review, which provides information about basic anatomy of the human shoulder joint as well as common conditions of the shoulder. Further, this chapter describes treatment options for these conditions and complications that may arise from some of these treatments. This chapter also discusses anatomical considerations when designing stem prostheses for the proximal humerus. Finally, an overview of statistical shape modeling is given.

Chapter 3 provides a description of how the information was processed, including a description of the training set, which software was used, methods used to develop the training set data, and the method used to develop the statistical shape model.

Chapter 4 is a presentation of the results including Leave-One-Out analysis, principal components, and anatomical measurement correlations.

Finally, Chapter 5 includes discussions of those results, their significance, limitations of the study, as well as potential future work.

CHAPTER 2: A REVIEW OF LITERATURE

This chapter will cover the anatomy of the shoulder joint, conditions that affect the shoulder, treatments for shoulder conditions, reasons for primary shoulder replacement surgery, reasons for revision shoulder surgery, and considerations when designing a shoulder stem prosthesis. Finally, this chapter will cover the some prior use of Statistical Shape Modeling (SSM) and the use of SSM in this thesis.

2.1 Anatomy of the Shoulder

The shoulder consists of three bones (Fig. 2.1): the humerus (upper arm bone), the scapula (shoulder blade), and the clavicle (collar bone). The shoulder consists of four joints: the sternoclavicular joint, the scapulothoracic joint , the acromioclavicular joint, and the glenohumeral joint. Of these, the acromioclavicular joint and the glenohumeral joint are the two main joints that help the shoulder move. The acromioclavicular joint is located between the clavicle and a bony process on the scapula, called the acromion. The glenohumeral joint, commonly called the shoulder joint, is between the socket of the scapula, also called the glenoid, and the “ball” or “head” at the top of the humerus (Fig. 2.2).

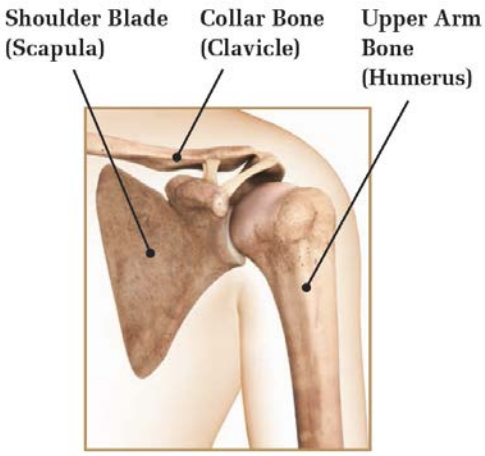

Figure 2.1: Bones of the shoulder (DePuy Synthes 0612-81-510).

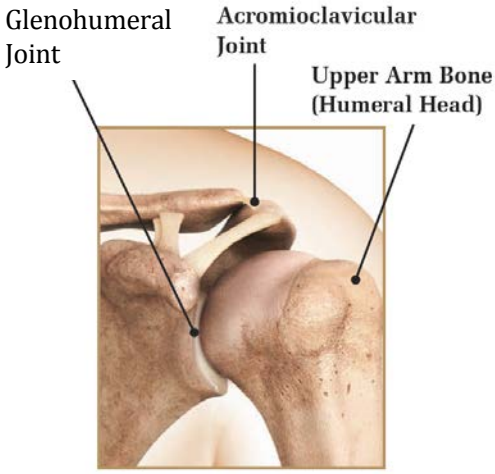

Figure 2.2: Glenohumeral joint – between the glenoid and humeral head, and acromioclavicular joint – between the clavicle and acromion (DePuy Synthes 0612-81-510).

The surface area contact relationship between these two bones of the glenohumeral joint is similar to a golf ball sitting on a golf tee. A sophisticated arrangement of muscles, tendons and ligaments support these bones to constrain and control movement in the shoulder, making it one of the more complex joints in the body. These soft tissues include the labrum, the rotator cuff, and the bursa. The labrum is a ring of cartilage surrounding the glenoid which forms a cup in which the humeral head can ride. It helps provide shoulder stability. The rotator cuff is a collection of muscles and tendons that surround the shoulder. The four muscles of the rotator cuff are the supraspinatus, infraspinatus, subscapularis, and teres minor. The rotator cuff provides support to the shoulder and upper arm while providing a wide range of motion. Finally, the bursa is a small synovial membrane containing synovial fluid that helps protect the tendons of the rotator cuff and reduce

friction. This relatively loose fit and complex arrangement of soft tissue results in the shoulder having the largest range of motion of all of the joints in the human body (Fig. 2.3).

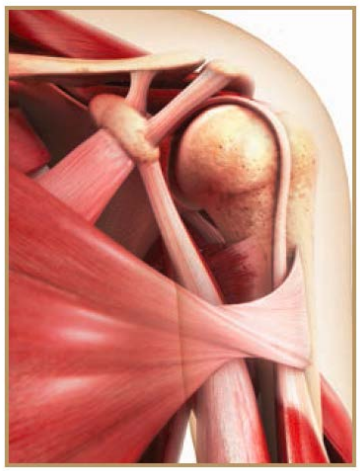

Figure 2.3: Soft tissues of the shoulder (DePuy Synthes 0612-81-510).

2.2 Shoulder Conditions

Most shoulder problems involve the muscles, tendons, or ligaments of the shoulder, but the bones can also be affected. These include arthritis, torn rotator cuff, dislocation, instability, frozen shoulder (adhesive capsulitis), sports injuries, synovitis, tendinitis, bursitis, impingement syndrome, and fractures.

According to the Centers for Disease Control and Prevention, the number one cause of disability in the United States is arthritis. Approximately one in every three Americans suffers from some form of arthritis (CDC, 2009). Arthritis is the loss of hyaline cartilage, which is the smooth, shiny surface that covers the articulating surface of epiphyses to reduce friction during joint movement (Fig. 2.4). In healthy bones there is smooth and painless motion when bones articulate together. However, when cartilage

degenerates, pain often follows and the supporting soft tissues can become weak resulting in reduced motion.

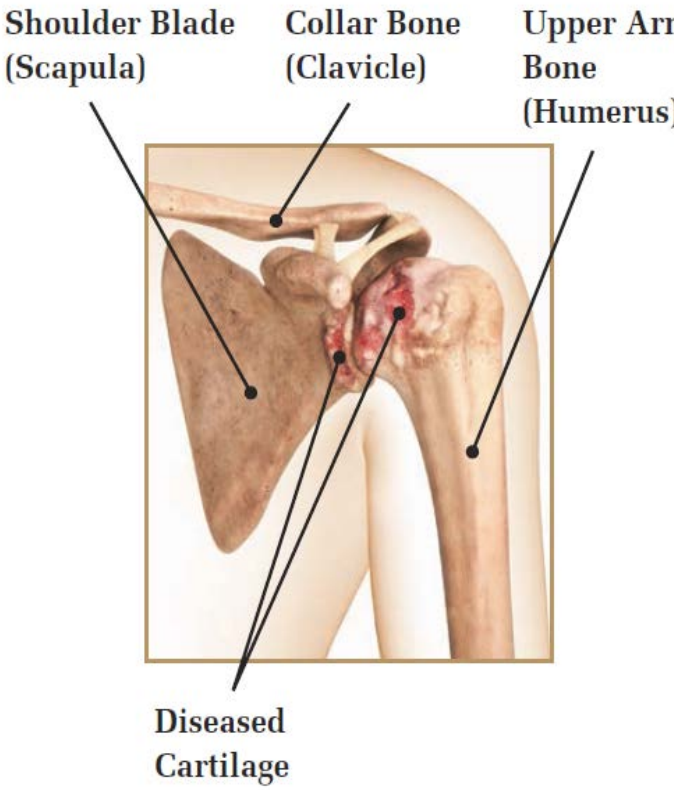

Figure 2.4: Example of an arthritic shoulder (DePuy Synthes 0612-81-510).

Three main types of arthritis generally affect the shoulder: osteoarthritis, rheumatoid arthritis, and arthritis related to trauma. Other forms of less common arthritis that can affect the shoulder include septic arthritis resulting from infection, and avascular necrosis resulting from a disrupted blood supply.

2.2.1 Arthritis

Osteoarthritis occurs when the hyaline cartilage protecting the articulating surface deteriorates over time and loses the ability to repair itself. When this occurs, cartilage loss, bone damage, the formation of bone spurs, and soft tissue inflammation can occur. Rheumatoid arthritis destroys the hyaline cartilage and the synovial lining covering the joint capsule through severe inflammation. Rheumatoid arthritis affects all ages and more females than males. It can also affect all joints in the body. Arthritis that results from damage caused by a previous injury to the joint is called trauma-related arthritis. Like the other types of arthritis, trauma-related arthritis can result in pain, damage to the joint, and the loss of joint mobility.

2.2.2 Other Shoulder Conditions

Gout is another form of arthritis in which crystals form in the joint. While gout can occur in the shoulder, causing inflammation and pain, it is more common in other joints of the body. Frozen shoulder develops as the movement becomes severely limited due to pain and stiffness caused by inflammation. If the acromion interferes with the rotator cuff when the arm is lifted this is referred to as shoulder impingement. This can be painful if inflammation is present. Exercises to strengthen the rotator cuff can sometimes help reduce shoulder impingement. A rotator cuff tear is a tear in one of the rotator cuff muscles or tendons that may result from a sudden injury, such as a fall, or from steady overuse, such as throwing a ball. Shoulder tendonitis occurs when a tendon of the rotator cuff becomes inflamed but is not torn. A labral tear is a tear in the ring of cartilage that surrounds the

glenoid, called the labrum. It can be caused by a sudden injury or by overuse. Shoulder bursitis occurs when the bursa becomes inflamed, causing pressure on the upper arm and pain with overhead activities. Finally, a shoulder dislocation occurs when the humeral heads slips out of position in the glenoid fossa. In younger people this is often caused by a sports related incident. Unlike shoulder dislocation, which affects the glenohumeral joint, shoulder separation involves the acromioclavicular joint. A separation can damage the joint, the cartilage inside, and the ligaments that maintain stability.

2.3 Shoulder Treatments

There are a number of options for the treatment of shoulder issues. These range from home treatments such as RICE - a combination of rest, ice, compression, and elevation - and over the counter pain relievers anti-inflammatories, to treatments that require medical direction such as prescription pain relievers, corticosteroids, and physical therapy, to more invasive treatments such as arthroscopic surgery, fracture repair surgery, and shoulder replacement option. If pain and stiffness continue after home treatments are tried, or if pain is severe, then a physician is often consulted.

2.3.1 RICE

RICE is often the first treatment steps for shoulder pain. RICE can often improve the pain and swelling for many shoulder injuries. Rest means to simply stop using the injured area for a couple of days. Ice includes using a cold pack wrapped in a towel on the affected area several times a day for short periods. Compression may help reduce any swelling by compressing the affected area with elastic bandages. Compression is often not

necessary. Finally, Elevation refers to keeping the affected area raised above the level of the heart.

2.3.2 Medication

Shoulder pain is a reminder that there is an issue with the shoulder and over-the-counter or prescription pain medication may help with this symptom. Non-steroidal anti-inflammatory drugs (NSAIDS) are medications that combine pain relievers with anti-inflammatories and can be purchased through a prescription or over-the-counter, such as ibuprofen. Non-NSAIDs, such as acetaminophen, do not reduce inflammation and are over the counter medications. Corticosteroids are prescription anti-inflammatory medications that block the production of prostaglandins that trigger pain and inflammation. These come in medication form or can be injected directly into the shoulder by a healthcare professional.

2.3.3 Physical Therapy

Physical therapy involves a series of mobility and strengthening exercises designed to reduce pain and restore flexibility in the shoulder. It can be used as a primary treatment option or for post-surgery rehabilitation and will be recommended and/or supervised by a doctor or physical therapist.

2.3.4 Surgery

Surgery is generally performed to make the shoulder more stable or when severe shoulder pain starts interfering with daily activities. Different surgical treatment options include arthroscopic surgery, shoulder resurfacing, rotator cuff-tear arthropathy (CTA)

surgery, reverse shoulder replacement, shoulder fracture repair and total shoulder replacement.

2.3.4.1 Arthroscopic Surgery

In arthroscopic surgery, or arthroscopy, a surgeon makes small incisions in the shoulder and performs surgery through a flexible tube with a camera and tools on its end called an endoscope. It can be used to diagnose and treat shoulder problems such as a torn rotator cuff, shoulder impingement, shoulder instability, arthritis, tendonitis and bursitis. Arthroscopic surgery is minimally invasive in nature and requires less recovery time than open surgery.

2.3.4.2 Partial and Total Shoulder Replacement

The first anatomic design of a vitallium humeral head was introduced by Krueger in 1951, thus beginning the era of shoulder arthroplasty as a treatment option (McPherson et al., 1997; Krueger et al., 1951). It may be time to consider shoulder replacement if medications, physical therapy and other methods of treatment no longer relieve pain. The intent of shoulder joint replacement is to reduce pain and improve joint mobility. According to the Agency for Healthcare Research and Quality (AHRQ), joint replacement will become the most common elective surgery by the year 2030 (AHRQ, 2016).

During total shoulder replacement surgery, or total shoulder arthropathy (TSA), the worn or affected portions of the shoulder are replaced with components designed to function with the human anatomy and function as close to natural human movement as possible. The main components of a TSA surgery are the humeral head, the stem, and the

glenoid component. The head of the humerus is replaced by metal head of similar size and radius. This component is often made of a biocompatible cobalt chrome alloy because this surface will articulate with the glenoid component and this material has superior wear properties. A metal stem is often made of a titanium alloy because of this material's strength to weight ratio, and is fit into the canal of the humerus to give the implant sufficient stability. The humeral head is often attached to the humeral stem by a locking taper or threaded connection. Finally, the glenoid component is often made of high-strength polyethylene and the geometry of the articulating surface is selected based on the size of the humeral head. The glenoid component is attached to the scapula using bone cement and/or bone screws (Fig. 2.5).

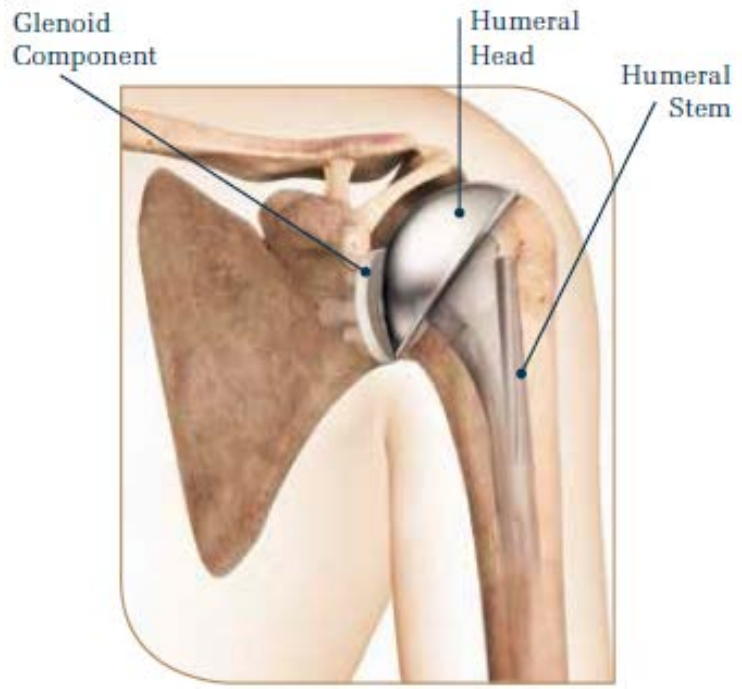

Figure 2.5: Example of a total shoulder replacement (DePuy Synthes 0612-76-510).

The surgeon will often determine which implant components and which sizes might be needed with preoperative planning using patient x-rays. During surgery, the surgeon will determine final sizing of the implant based on fit into the bone and "trialing" where the stability and range of motion of the joint are checked. The sizes of each component may vary to best match the anatomy of the patient. If all three of the main components are used it is considered a total shoulder replacement. If only the humeral head and/or the glenoid component are used then it is considered a partial shoulder replacement.

Joint registries have been established in some countries to collect information on joint replacement surgeries with a goal of maintaining or improving outcomes for patients. These registries are generally ran or funded by the government of the country and track the surgeries that take place within their country. Two well established national registries are the National Joint Registry (NJR) in the United Kingdom, and the Australian Orthopaedic Association National Joint Replacement Registry (AOANJRR). Variations in data between registries can sometimes be seen due to numerous contributors, including variations in care practices between geographic regions.

When a patient has a joint replacement surgery for the first time it is categorized as a "primary" surgery. Any subsequent surgeries due to complications from the primary surgery are classified as "revision" surgeries. According to the AOANJRR 2016 Annual Report, 94.1% of primary total shoulder replacement surgeries were due to osteoarthritis (Table 2.1).

Table 2.1: Reasons for primary total shoulder replacement (AOANJRR 2016 Annual Report, 292).

Table ST18 Primary Total Conventional Shoulder Replacement by Primary Diagnosis and Gender

	Male		Female		TOTAL	
Primary Diagnosis	N	Col%	N	Col%	N	Col%
Osteoarthritis	4065	95.6	5559	93.0	9624	94.1
Rheumatoid Arthritis	52	1.2	145	2.4	197	1.9
Osteonecrosis	36	0.8	117	2.0	153	1.5
Fracture	22	0.5	81	1.4	103	1.0
Other Inflammatory Arthritis	21	0.5	36	0.6	57	0.6
Rotator Cuff Arthropathy	31	0.7	18	0.3	49	0.5
Instability	18	0.4	12	0.2	30	0.3
Tumour	4	0.1	5	0.1	9	0.1
Other	5	0.1	3	0.1	8	0.1
TOTAL	**4254**	**100.0**	**5976**	**100.0**	**10230**	**100.0**

2.3.4.3 Shoulder Resurfacing

Shoulder resurfacing is considered a more conservative alternative to traditional shoulder replacement surgery. In a resurfacing procedure only the diseased surfaces of the effected joint are removed. This results in retention of more natural bone. The removed surface of the humeral head is replaced with a metal implant that covers the articulating surface (Fig. 2.6). If needed, this less invasive approach may allow a patient to have a total replacement later.

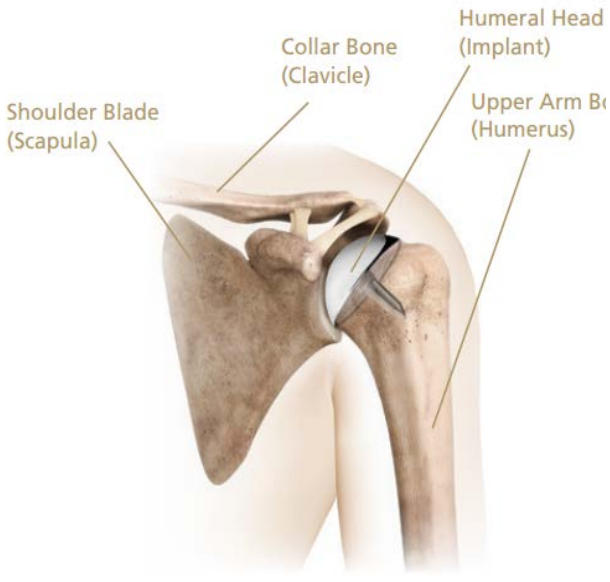

Figure 2.6: Example of shoulder resurfacing (DePuy Synthes 0612-77-510).

A fourteen year study by Levy and Copeland looked at 94 patients who had shoulder resurfacing surgery for treatment of the following: osteoarthritis, rheumatoid arthritis, avascular necrosis, instability arthropathy, post-traumatic arthropathy, and cuff arthropathy. Of the 94 patients, 93.9% felt that the shoulder was much improved or improved after the surgery, with the best results coming from those who had been treated for primary osteoarthritis, and the poorest results were seen in patients with cuff arthropathy and post-traumatic arthropathy (Levy et al., 2001).

A more recent study published in 2008 assessed pain, function, and patient satisfaction, as well as implant loosening, in resurfacing patients under the age of 55. Of the 36 patients, thirty-five patients were satisfied with the outcome and had returned to their desired activity level (Bailie et al., 2008).

Osteoarthritis is the primary diagnosis leading to resurfacing. According to the AOANJRR 2016 Annual Report, 94.9% of primary shoulder resurfacing surgeries were due to osteoarthritis (Table 2.2).

Table 2.2: Reasons for shoulder resurfacing (AOANJRR 2016 Annual Report, 287).

Table ST8 Primary Total Resurfacing Shoulder Replacement by Primary Diagnosis and Gender

	Male		Female		TOTAL	
Primary Diagnosis	N	Col%	N	Col%	N	Col%
Osteoarthritis	118	95.9	70	93.3	188	94.9
Rheumatoid Arthritis	1	0.8	2	2.7	3	1.5
Fracture	1	0.8	1	1.3	2	1.0
Other Inflammatory Arthritis			1	1.3	1	0.5
Instability	1	0.8	.	.	1	0.5
Rotator Cuff Arthropathy			1	1.3	1	0.5
Osteonecrosis	1	0.8			1	0.5
Other	1	0.8			1	0.5
TOTAL	**123**	**100.0**	**75**	**100.0**	**198**	**100.0**

Note: Instability includes Instability and Dislocation

2.3.4.4 Cuff-Tear Arthropathy Repair

Rotator Cuff-Tear Arthropathy (CTA) is an arthritic condition that occurs due to thinning of the bone, or osteoporosis, or when there is a large rotator cuff tear over an extended period of time (Fig. 2.7). With CTA the rotator cuff muscles have become weak or non-functional and there is typically severe pain and very limited movement. Sometimes this can be alleviated by surgically repairing the tear in the muscle arthroscopically and in some cases a joint replacement is used.

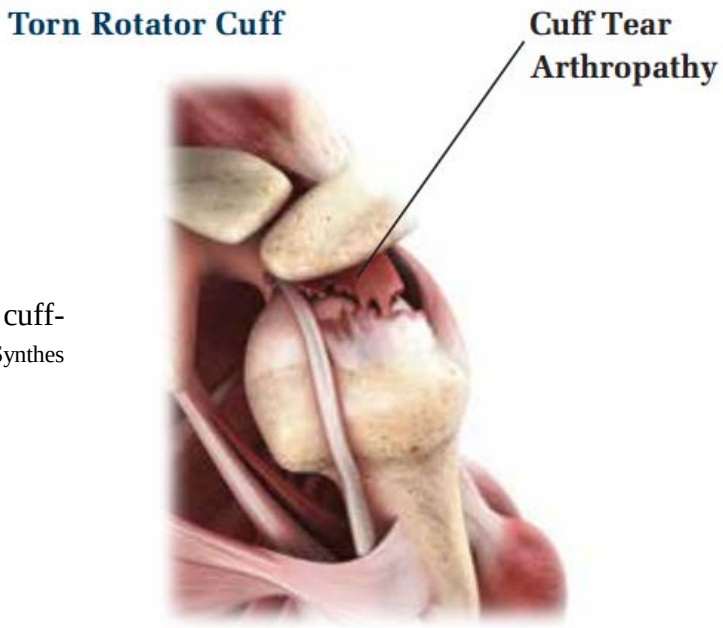

Figure 2.7: Example of cuff-tear arthropathy (DePuy Synthes 0612-79-510).

2.3.4.5 Reverse Shoulder Replacement

When all other treatment options have been exhausted for CTA, a reverse shoulder joint replacement can be successful. During a reverse shoulder replacement surgery the anatomy of the shoulder is reversed, allowing the deltoid muscle to do the majority of

lifting of the arm. Rather than the ball of the joint being at the end of the humerus it is instead placed on the glenoid area of the scapula. The cup is then instead placed at the proximal end of the humerus (Fig. 2.8). The joint of the shoulder is held together by altered mechanics and the damaged rotor cuff is not needed for lifting the arm.

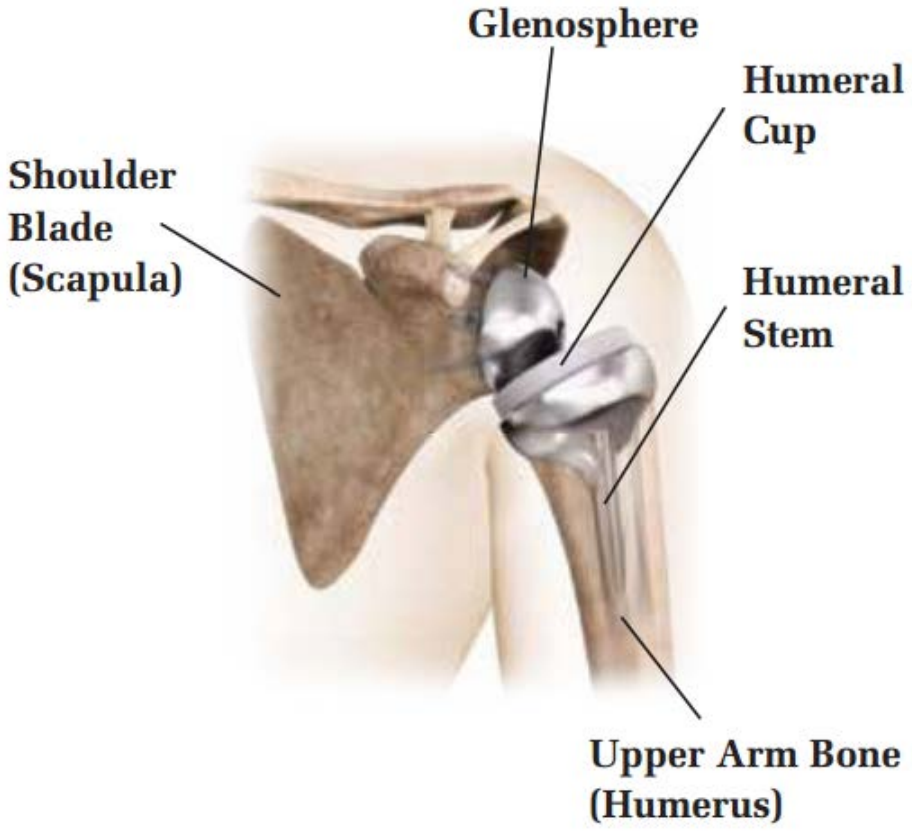

Figure 2.8: Example of a reverse shoulder replacement (DePuy Synthes 0612-79-510).

According to the AOANJRR 2016 Annual Report, 79.7% of primary reverse shoulder replacement surgeries were due to osteoarthritis or rotator cuff arthropathy. Fracture also leads to 14.6% of reverse shoulder replacements (Table 2.3).

Table 2.3: Causes of primary reverse shoulder replacement (AOANJRR 2016 Annual Report, 307).

Table ST33 Primary Total Reverse Shoulder Replacement by Primary Diagnosis and Gender

	Male		Female		TOTAL	
Primary Diagnosis	N	Col%	N	Col%	N	Col%
Osteoarthritis	2047	48.6	3584	44.0	5631	45.6
Rotator Cuff Arthropathy	1716	40.7	2495	30.6	4211	34.1
Fracture	264	6.3	1543	18.9	1807	14.6
Rheumatoid Arthritis	55	1.3	233	2.9	288	2.3
Instability	51	1.2	103	1.3	154	1.2
Osteonecrosis	23	0.5	110	1.4	133	1.1
Tumour	45	1.1	44	0.5	89	0.7
Other Inflammatory Arthritis	10	0.2	33	0.4	43	0.3
Other	3	0.1	3	0.0	6	0.0
TOTAL	**4214**	**100.0**	**8148**	**100.0**	**12362**	**100.0**

Note: Instability includes Instability and Dislocation

2.3.4.6 Fracture Surgery

Fracture surgery may be needed when a shoulder fracture occurs, or if the fracture does not heal properly. Shoulder fractures often occur when the hand is extended to stop a fall, resulting in a transferred force to the shoulder. This often results in a predictable fracture pattern in the proximal humerus (Fig. 2.9).

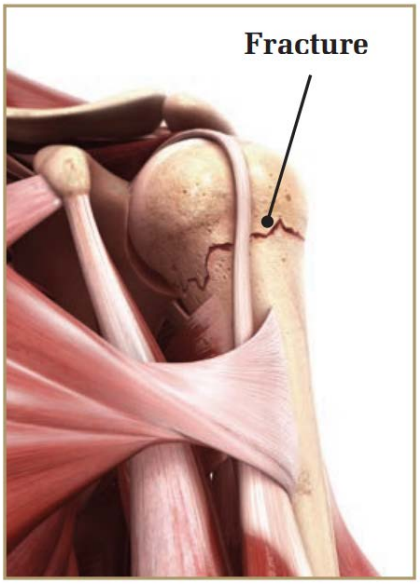

Figure 2.9: Example of a shoulder fracture (DePuy Synthes 0612-81-510).

The surgeon may decide to place the bone fragments in their natural position and allow them to repair, or the surgeon may suggest shoulder replacement surgery, especially if the proximal humerus is severely broken or crushed. Fracture shoulder prostheses are designed with features that allow for repair and healing of the broken bone, to help restore motion and reduce pain.

The AOANJRR classifies a surgery which involves a resection of the humeral head and a replacement with a stemmed humeral prosthesis and a humeral head prosthesis as a "hemi stemmed" surgery. Hemi stemmed surgeries account for 74.8% of all partial shoulder replacements (AOANJRR 2016, 260). According to the 2016 AOANJRR Annual Report, 46.6% of partial shoulder replacement surgeries were due to fracture (Table 2.4).

Table 2.4: Reasons for primary partial shoulder replacement (AOANJRR 2016 Annual Report, 262).

Table SP4 Primary Partial Shoulder Replacement by Primary Diagnosis and Gender

	Male		Female		TOTAL	
Primary Diagnosis	N	Col%	N	Col%	N	Col%
Fracture	573	28.9	2137	55.8	2710	46.6
Osteoarthritis	1064	53.7	1225	32.0	2289	39.4
Rotator Cuff Arthropathy	108	5.4	163	4.3	271	4.7
Osteonecrosis	63	3.2	98	2.6	161	2.8
Tumour	59	3.0	52	1.4	111	1.9
Rheumatoid Arthritis	15	0.8	87	2.3	102	1.8
Dislocation	27	1.4	37	1.0	64	1.1
Instability	47	2.4	13	0.3	60	1.0
Other Inflammatory Arthritis	10	0.5	12	0.3	22	0.4
Hill-Sachs Defect	14	0.7	4	0.1	18	0.3
Osteochondritis Dissecans	2	0.1			2	0.0
Other			2	0.1	2	0.0
TOTAL	**1982**	**100.0**	**3830**	**100.0**	**5812**	**100.0**

Note: Includes two humeral ball procedures

2.4 Complications with Shoulder Arthroplasty

While many thousands of patients have experienced an improved quality of life after primary shoulder joint replacement surgery, including less pain, improved motion and strength, and better function, occasional complications can occur from shoulder joint replacement. Some risks can include infection, implant loosening, pain, implant wear, dislocation, and nerve damage (AAOS, 2017). Occasionally the surgeon will treat the more severe cases with complications through a revision surgery in which an attempt will be made to alleviate the unwanted condition or replace the prosthesis. Revisions surgeries can be more complicated than primary surgeries as bone and soft tissue conditions have often deteriorated.

A failed shoulder arthroplasty can be defined as a complication, the need for a revision surgery, or by patient dissatisfaction. Characteristics of this dissatisfaction include stiffness, impaired function, and instability, related to loose or malpositioned components, glenoid erosion, and non-union of fractured tubersosities (Hasan et al., 2002).

According to the AOANJRR 2016 Annual Report the main type of revision shoulder surgery is when the humeral head components is replaced. In 82.1% of procedures the humeral stem is not revised (AOANJRR 2016, 294).

The majority (63.6%) of shoulder replacement revision surgeries were due to instability or dislocation, rotator cuff insufficiency, and loosening or lysis. Lesser occurring reasons for revision shoulder surgeries with causes associated with the prosthesis include implant breakage, implant sizing, malposition, and implant wear (Table 2.5).

Table 2.5: Reasons for revision shoulder surgery (AOANJRR 2016 Annual Report, 296).

Table ST22 Primary Total Conventional Shoulder Replacement by Reason for Revision

Reason for Revision	Number	Percent
Instability/Dislocation	168	25.2
Rotator Cuff Insufficiency	140	21.0
Loosening/Lysis	116	17.4
Implant Breakage Glenoid Insert	57	8.5
Infection	41	6.1
Dissociation	29	4.3
Implant Breakage Glenoid	19	2.8
Incorrect Sizing	15	2.2
Fracture	13	1.9
Arthrofibrosis	12	1.8
Pain	11	1.6
Metal Related Pathology	10	1.5
Malposition	6	0.9
Wear Glenoid Insert	4	0.6
Wear Glenoid	1	0.1
Glenoid Erosion	1	0.1
Other	24	3.6
TOTAL	**667**	**100.0**

To help determine if these revisions associated with the devices are due to something inherent in the design, the registries track revision surgeries by the product. This way it can be seen if a product has a higher revision rate than the other products that are within the same classification (Table 2.6). For example, table 2.6 shows that at one year after surgery the SMR shoulder prosthesis has a higher revision rate at 6.2% than other products in this class (0% to 4.4%), and this gap widens over time. At seven years after implantation the SMR product has a 19.0% revision rate, while the revision rate for the remainder of the class ranges from 3.3% to 6.2%.

Table 2.6: Shoulder revision rates by brand of prosthesis (AOANJRR 2016 Annual Report, 205).

Table ST31 Cumulative Percent Revision of Primary Total Conventional Shoulder Replacement by Prosthesis Combination (Primary Diagnosis OA)

Humeral Stem	Glenoid	N Revised	N Total	1 Yr	3 Yrs	5 Yrs	7 Yrs	9 Yrs
Aequalis	Aequalis	42	1543	1.3 (0.8, 2.0)	2.5 (1.8, 3.4)	2.9 (2.1, 4.0)	4.1 (2.7, 6.0)	
Aequalis Ascend	Aequalis	0	200	0.0 (0.0, 0.0)				
Affinis	Affinis	10	168	0.0 (0.0, 0.0)	1.8 (0.6, 5.6)	5.8 (2.9, 11.4)		
Ascend	Aequalis	6	264	0.8 (0.2, 3.3)	3.2 (1.4, 7.2)			
Bigliani/Flatow	Bigliani/Flatow	8	140	2.2 (0.7, 6.5)	3.7 (1.5, 8.6)	3.7 (1.5, 8.6)	6.2 (2.9, 13.0)	
Bigliani/Flatow TM	Bigliani/Flatow	19	340	2.5 (1.3, 4.9)	5.1 (3.1, 8.3)	6.5 (4.1, 10.3)		
Bigliani/Flatow TM	Bigliani/Flatow TM	20	500	2.8 (1.6, 4.8)	4.3 (2.7, 6.8)	4.7 (3.0, 7.4)		
Comprehensive	Comprehensive	6	163	4.4 (2.0, 9.5)				
Equinoxe	Equinoxe	2	110	1.1 (0.2, 7.9)				
Global AP	Global	57	2215	1.6 (1.1, 2.2)	2.7 (2.1, 3.6)	2.9 (2.2, 3.8)	3.6 (2.6, 5.0)	
Global Advantage	Global	22	551	1.5 (0.7, 3.0)	3.6 (2.3, 5.6)	3.6 (2.3, 5.6)	5.1 (3.3, 7.7)	
Global Advantage	Global Advantage	0	59	0.0 (0.0, 0.0)				
Global Unite	Global	1	200					
SMR	SMR	385	2623	6.2 (5.4, 7.3)	13.7 (12.3, 15.2)	17.8 (16.2, 19.6)	19.0 (17.2, 20.9)	
Solar	Solar	6	169	0.6 (0.1, 4.1)	2.4 (0.9, 6.3)	3.3 (1.4, 7.9)	3.3 (1.4, 7.9)	
Turon	Turon	1	60	1.7 (0.2, 11.2)				
Other (30)		33	319	3.6 (2.0, 6.5)	8.1 (5.5, 12.0)	11.1 (7.8, 15.6)	13.5 (9.5, 19.0)	
TOTAL		**618**	**9624**					

Note: Only combinations with over 50 procedures have been listed

To reduce product issues, regulatory bodies require extensive proof of robust testing or proof of equivalency to devices that already demonstrate clinical success. In some cases clinical trialing is required before the product is allowed to be released to market. Regulatory bodies also require companies that produce medical devices to execute a post-market surveillance plan to monitor complaints received and take corrective actions if needed. These governing bodies can also require products be removed from the market and not be sold if they feel there is an issue with the device that is not being resolved. Even with this published registry data, it can be challenging based off of this data alone to determine if the product design is causing this higher revision rate, or if some other cause or causes are driving this correlation. Further breakdown of the data can be requested from the joint registry to assist in these investigations.

2.5 Anatomical Considerations When Designing A Stem Prosthesis for the Proximal Humerus

When designing a shoulder stem prosthesis to fit in the proximal humerus consideration should be given to the changing anatomical features of the bone. During shoulder replacement surgery, size of the stem prosthesis is based off of fit within the cortices of the humerus, among other considerations, and resections are made from references to boney anatomic landmarks (Fig. 2.10).

As the size of the humerus and the size and location of these landmarks may change from patient to patient, designing a device or family of devices that function properly, meet the size range of the wider population, and are still cost effective to manufacture, can be challenging.

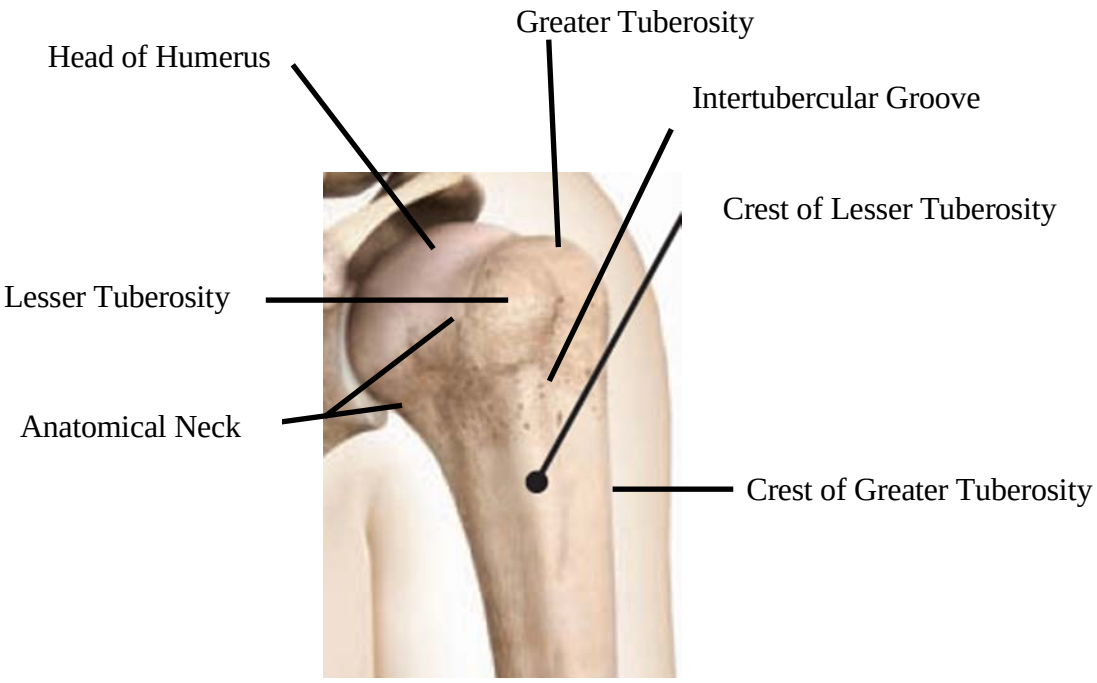

Figure 2.10: Anatomy of the proximal humerus (DePuy Synthes 0612-81-510).

Challenges of designing a robust implant and surgical procedure with regards to interaction with the patient are numerous. Some of these include maintaining sterility, the biocompatibility of the device, fitting the device to the patient anatomy, and designing prosthesis components to mate and work together.

If the implant is not properly adapted to the patient's anatomy, or improperly fits with the bone, this can result in pain, loosening of the prosthesis, poor joint mechanics, or damage to the bone. Similarly, if there is inadequate implant fixation from a lack of press fit between the stem and epiphyseal body, or if the device does not properly adhere to the bone, this can result in pain or loosening of the device. Conversely if there is too much press fit into the bone between the stem and epiphyseal body this can lead to bone fracture or an improper sizing of the implant which can result in pain, user dissatisfaction, soft tissue irritation or poor joint mechanics. And while not directly related to bone anatomy and implant fit, a non-sterile device can lead to infection and using materials which aren't biocompatible can lead to an adverse tissue reaction. Any of these complications can lead to user dissatisfactions or, if very severe, can result in a revision surgery.

Ensuring that the components of a prosthesis mate with each other or work properly together is often easily verified, but validating how the device interacts with the patient anatomy can be more challenging to confirm. For example, a tolerance analysis or drawing review might be used to confirm the proper mating conditions between components, and laboratory testing can easily confirm the pull-off strength of a locking taper junction. But confirming that a device fits properly within a patient's anatomy, such as determining

whether a screw will engage with cortical or cancellous bone when the implant is properly fit, or whether a drill or reamer will perforate the cortex of the bone, is often validated in cadaveric specimens and these are limited to sizes of specimens that are available. So validating that a device system fits a wider, global population could be time consuming and cost prohibitive. Knowing if and how the boney landmarks, anatomic neck and the size and shape of the intramedullary canal change across a patient population can be helpful in designing a humeral stem prosthesis that will meet the needs of a broader population, or in designing a system specific to a subset of a population or a specific ethnic group. Historically this has been done collecting numerous two-dimensional x-rays or CT scans and taking measurements to predict the span of sizes of implants that might be needed. Therefore the use of SSM to create a three-dimensional bone construct by which to design a prosthesis for a broad or specific patient population can be very efficient and robust.

2.6 Statistical Shape Modeling

Statistical shape modeling (SSM) is a method of using point distribution model to establish point correspondence between a training data set and a subject data set, and then make a statistical analysis of the variation between the sets (Cootes et al., 1995). One of the main steps used in SSM is principal component analysis (PCA). After nodes of subject models are registered, PCA is a method in which the variability in data is characterized using common modes of variation to define the inconsistencies in a set of corresponding points (Jolliffe, 2002). In addition to principal component analysis, other algorithms used in SSM include iterative closet point, coherent point drift, and leave one out analysis.

Iterative Closest Point (ICP) algorithms have been used to calculate the differences between two sets of data points by estimating the difference between a point and another nearby point, then calculating the rotation and translation to achieve the consolidation of the point location, and then performing the transformation while minimizing root mean square distance between the surfaces (Besl, 1992; Zhang, 1994). This has previously been used to align to align and register bone models (Zheng et al., 2009).

Coherent Point Drift (CPD) is a probabilistic method to estimate complex non-linear non-rigid transformations, and can be used the registration of point sets. The CPD method simultaneously finds both the non-rigid transformation and the correspondence between two point sets. When tested using outlying data points or having data points removed, CPD has been shown to be robust and accurate on both 2D and 3D examples (Myronenko, 2010).

Leave One Out (LOO) is a method of cross-validation, sometimes called rotation estimation (Geisser, 1993), that is used to assess the accuracy of a statistical shape model – the ability to describe a new or left out subject. This technique is used to estimate how accurately the predictive model will perform when there is not enough data available to partition it into separate training and test sets without losing significant modelling or testing capability (Grossman et al., 2010). One data sample is left out while computation is done on the remaining samples. LOO has been used previously to assess the robustness of statistical shape-function models of the knee joint (Fitzpatrick et al., 2011.)

Statistical shape models have been used widely in a variety of fields to characterize variation within a data set and predict a new instance from, and among, the data set. In the field of orthopedic implant design, sizing for a broad population has historically been based on two-dimensional analysis from medical imaging to drive clinical decision making (Hertel et al., 2002; Boileau and Walch, 1997; Humphrey et al., 2016). In human anatomy SSMs have been used to describe the changes variability in the bone morphology for training sets of subjects representing a wider population (Rao, 2013). Meller and Kalendar (2004) created an SSM for the pelvis, Bryan et al. (2010) and Bredbenner et al. (2008) for the knee, and Kamer et al. (2016) and Yang et al. (2008) for the shoulder.

In the area of the shoulder joint, Yang et al. presented a technique to derive the morphological relationship between the scapula and humerus bones and a method to predict one bone shape efficiently from the other using partial least squares regression (2008). Mutsvangwa et al. have developed methods to assess the shape of the cortical bone regions of the humerus and scapula. The cancellous bone regions were not considered. (2015). Drew et al. used SSM of the humerus to look at variability of the both the humerus endosteal and periosteal surfaces for rapid endoprosthetic stem design iteration (2014). Kamer et al. utilized a large number of subjects (58) and analyzed variation in size and shape, as well as bone density distributions. However, this study did not investigate differences in ethnicity or gender (2016).

The objective of this study was to develop a SSM of the cortical and cancellous bone regions of the proximal humerus, and to assess potential shape differences with

gender and ethnicity. The goal would then be utilize this information in the design of humeral implants and surgical instrumentation.

CHAPTER 3: METHODS

3.1 Population Selection: Training set

The present analysis uses a statistical shape model to describe the anatomical variation in cortical and cancellous bone geometry for a training set of selected CT scans. The training set included sixty-three cadavers or living subjects (Appendix A), which included twenty-nine females and thirty- four males. Ethnic groups included two African-American subjects, thirty Caucasian subjects, twenty Japanese subjects and eleven Taiwanese subjects. A bone with a median humeral head size was chosen as the template subject.

Age for the entire population of subjects ranged from thirty years to ninety-six years. Female subjects ranged from age thirty years to ninety-six years, while male subjects ranged from ages forty-four to ninety-two (Table 3.1).

Table 3.1: Subject age data.

Subject Age Data	Caucasians	Asians	African Americans	Males	Females	Caucasian Females	Asian Females	Caucasian Males	Asian Males
Average Age	75.6	70.1	73.0	72.7	76.7	80.7	70.1	77.0	70.2
Std Dev - Age	12.7	14.1	0.0	13.1	13.7	9.8	16.9	14.1	12.8
# of Subjects	30	31	2	35	28	17	11	13	20

Height, weight, and Body Mass Index (BMI) were collected for the Caucasian subjects only. Height of Caucasian subjects varied from 60” to 77” while weight ranged from seventy pounds to two hundred and fifty pounds. BMI for the Caucasian subjects ranged from 11.62 to 34.86% (Table 3.2).

Table 3.2: Caucasian subject data.

	Caucasians
Average Age (Years)	79.2
Std Dev - Age	11.6
Average Height (Inches)	66.2
Std Dev - Height	4.4
Average Weight (Pounds)	134.6
Std Dev - Weight	36.3
BMI	21.0
Std Dev - BMI	6.9
# of Subjects	30

3.2 Data Processing

3.2.1 Segmentation

Segmentation was performed on each humerus by first loading the raw CT DICOM data into Mimics (Materialise, Leuven, Belgium). A region grow operation was used to separate the humerus and scapula into two masks. Next cortical bone was separated from cancellous bone using a series of steps. A cortical mask was created and thresholding was

initiated. The erase and draw operations were used and initial threshold values were set to initiate the separation of cortical bone. Next polylines were calculated and cavity fill was executed using the polylines to encompass the boundaries of the cortical humerus. The erase, draw and threshold commands were then executed again on the separated cortical bone to complete the cortical mask. Finally, the calculate 3D command was executed to create a 3D construct of the cortical bone.

For the cancellous bone, the corresponding cortical model was eroded and a new mask was created using specified upper and lower Hounsfield Units (HU) limits. Boolean intersect was then executed on the new cancellous mask and the eroded cortical mask. Polylines were calculated and again cavity fill was executed from the polylines. The calculate 3D command was executed to create a 3D construct of the cancellous bone, and finally the construct was smoothed using the wrap 3D and smooth 3D operations. The construct was now ready for pre-processing (Fig. 3.1).

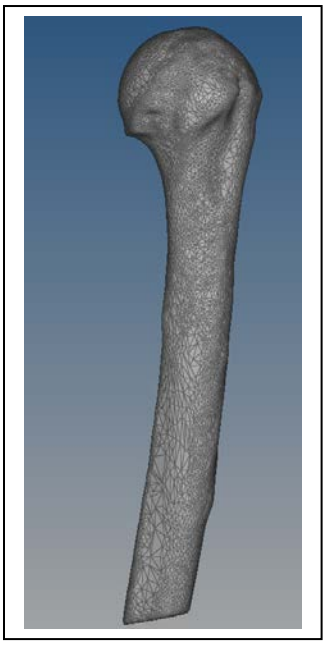

Figure 3.1: Example of a segmented proximal humerus.

3.2.2 Pre-Processing

The segmented stereolithography (STL) files containing the mesh with nodes and elements were pre-processed using HyperMesh (Altair, Troy, Michigan, USA). STL files representing both the cancellous and cortical components were imported into HyperMesh and given a new 2D automesh of the outer surface using 1mm trias elements. This replaced the mesh that was already on the STL file with a more uniform mesh. Next a surface was created using the new 2D elements for both the cancellous and cortical components for the purpose of cutting the humeri to a specified proportional length. This was done for consistency in the models since not all of the CT scans captured the full length of the humerus. Once the surfaces were created, the 2D mesh was deleted. A sphere was created with the center located at the head center of the humerus. The trim surface command was then used to cut both the cancellous and cortical components to the determined length, using the sphere as the cutting guide (Fig. 3.2).

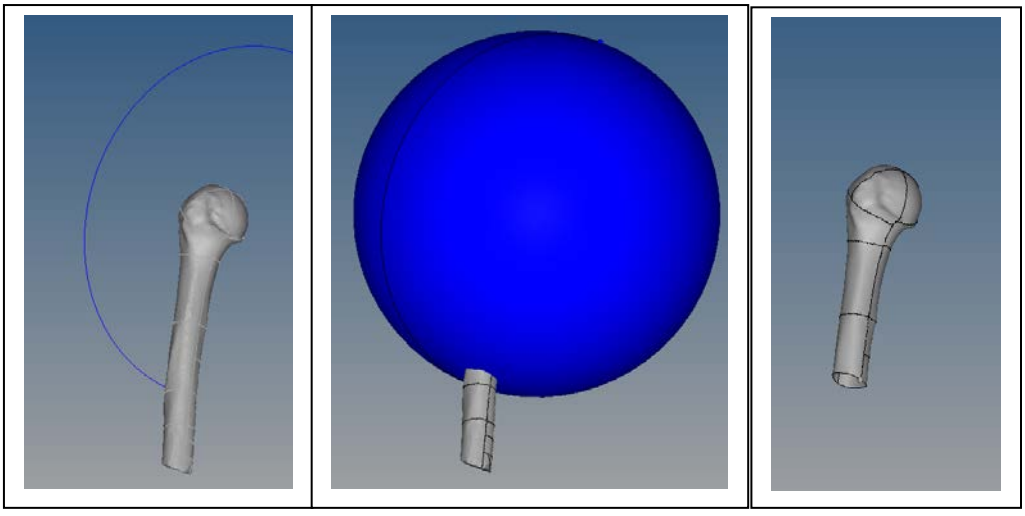

Figure 3.2: Trimming the humerus.

The radius of the sphere was 5.6 times the radius of the cortical head. This ratio was chosen to allow the humeri lengths to accept the full length of a standard shoulder stem prosthesis, and to still allow usage of a large population of the CT scans.

After the length of the humeri were set, all elements were converted to R3D3 using a Bolean option to make ready for exporting. For right-sided humeri, the Reflect command was used to change it to a left-sided humerus. This was needed so all humeri in the training set were of the same relative geometry in order to execute SSM. In doing this, an assumption of symmetry between left and right humeri of the same subject was assumed. All nodes and elements for both the cortical and cancellous bone were then renumbered and exported into folders.

The alignment of the subject model was compared to the template model and values for angle of rotation and translation to bring them into rough alignment were determined. These values were recorded to be used in the processing step.

3.2.3 Processing

Processing of the meshed input files using SSM was performed with a custom Matlab (Mathworks, Natick, Massachusetts, USA) script (Appendix C). Principal Component Analysis (PCA) was applied to data that represented both the cancellous and cortical humeral bone. Principal Components (PC) scores were used to represent the modes of variation that described the anatomic disparity present in the population data. A leave-one-out (LOO) analysis was utilized to evaluate the robustness of the SSM. Further details of these steps are described below.

After the cortical and cancellous bone models were manually rotated and translated in HyperMesh to have them roughly aligned with the training model, the template geometry was loaded into Matlab and all nodes and elements were renumbered and written to output files. The subject geometries were imported from HyperMesh as well, and nodes and elements were renumbered and written to output files.

An iterative Closest Point (ICP) algorithm was then used to minimize root mean square distance between the surfaces while performing a rigid body transformation to fully align the subject bones with the templates bones.

A Coherent Point Drift (CPD) algorithm was then used to apply a non-rigid transformation of each subject bone to the template bone. By morphing each subject to the template, it was determined which node of the template each node of the subject corresponds. This nodal correspondence from the non-rigid CPD was captured for subject registration, as was the correct position and orientation with respect to the template, creating a rigid body transformation matrix from the ICP. The cancellous bone was then re-aligned to the corresponding cortical bone.

A register was created to organize the subject data into columns, with each column representing a subject and each row representing x-y-z nodal coordinates. The values from the transformation matrices were added to the end of the nodal coordinate data in the register. The registered node coordinates from the rigid CPD matched total number of nodes as the template.

Prior to running the PCA, a model was created of each subject in the register using the nodal coordinate data to verify that the register contained the correct information. PCA was then executed and parallel analysis was used to understand which modes to retain. A mean model was created and new geometry was created and written to output files to visualize the modes of variation.

Anatomical measurements were calculated, and modes and anatomical measurements were analyzed by gender and ethnicity using Pearson's correlation coefficients. Measurements included head radius, medullary canal diameter, head sphericity, anatomical neck angle, greater tuberosity offset, articular surface thickness, inclination angle of the head, medial offset, anterior-posterior (AP) offset, and cortical thickness. Descriptions of how these measurements were made can be found in Appendix B.

Finally, a leave-one-out (LOO) analysis was performed to assess the accuracy of the SSM. The root mean square (RMS) error was determined by calculating distances from predicted nodes to the original nodes and then calculating the mean and standard deviation of the RMS errors.

CHAPTER 4: RESULTS

The SSM describes the anatomical variation with a series of modes of variation. In this chapter these modes of variation will be presented, as well as LOO analysis error. Further, the common mesh established by registration/correspondence enables anatomical measurements for all of the subjects. These measurements are relevant clinically and for implant design, and correlations between them will be included.

4.1 Modes of Variation

A series of modes of variation was used to describe variation in the humeral anatomy. The first three principal components accounted for 88% of the variation: PC1 explained 75% of variation, PC2 explained 10% of the variation, and PC3 accounted for 3% of the variation. Ninety-two percent of the variation was captured by the first five modes, with PC4 and PC5 each accounting for 2% of the variation (Fig. 4.1).

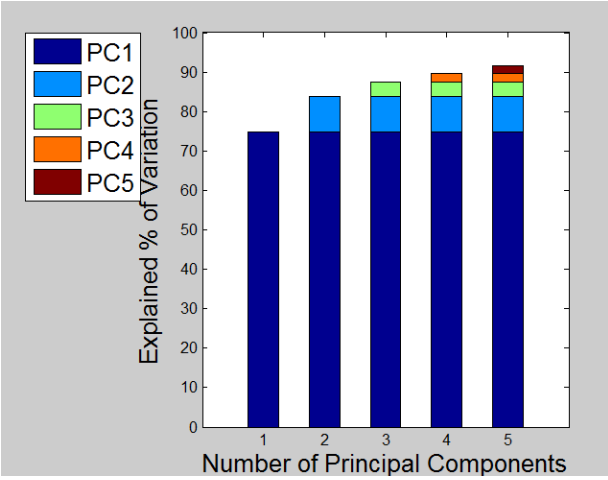

Figure 4.1: Principal components - % of variation.

The majority of the variability in the training set, or mode 1, was described by scaling of the bone. Changes near the lesser tubercle were described by mode 2. The radius of curvature of the medial side of the surgical neck, as well as changes in the greater tubercle, captured mode 3 (Fig. 4.2).

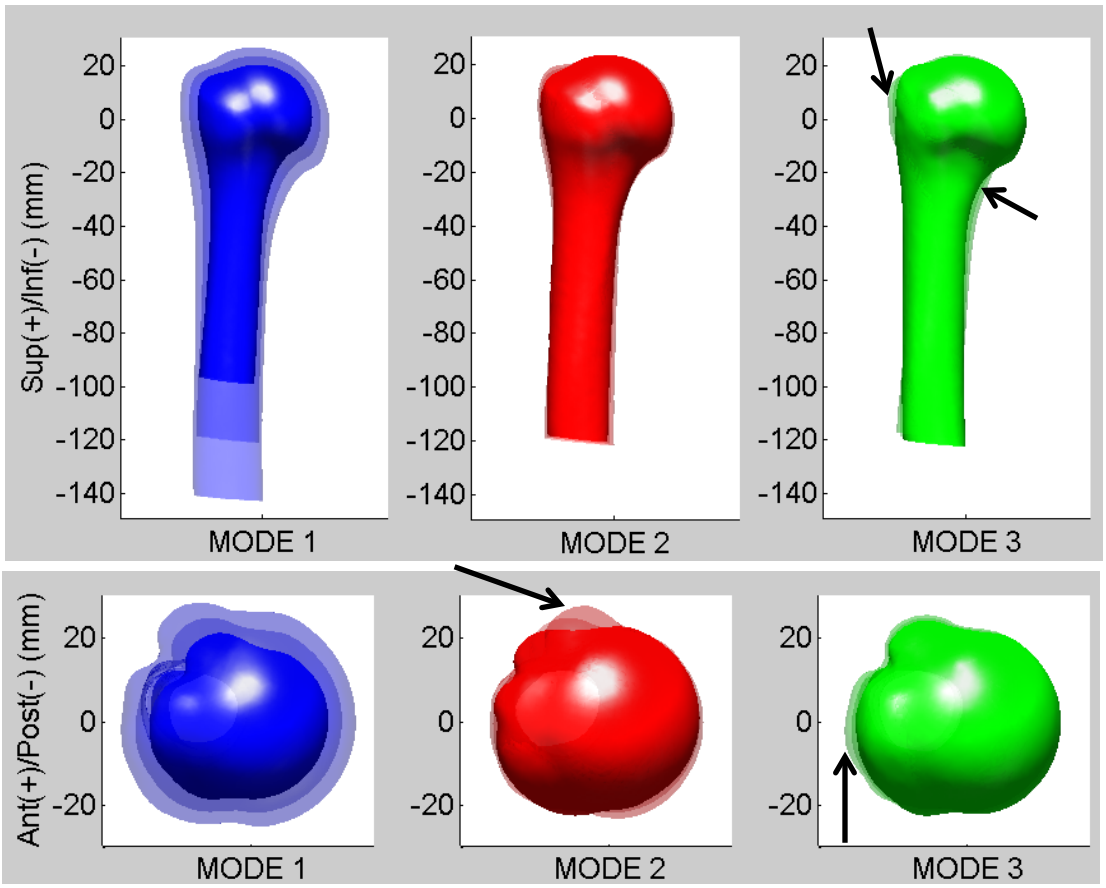

Figure 4.2: Principal components showing mean +/- 2 standard deviations.

4.2 Leave-One-Out Analysis

LOO analysis resulted in a root mean squared (RMS) error averaged across all nodes and all subjects of 0.89 mm with a standard deviation of 0.34 mm.

4.3 PC Correlations

Correlations help identify interactions between variables, and are a measure of sensitivity (Laz and Browne, 2009). Mode 1 was strongly correlated with humeral head radius (R=-0.96, Fig. 4.3), articular surface thickness (R=-0.90, Fig. 4.4), and greater tuberosity offset (R=-.82, Fig. 4.5). Mode 1 was also weakly correlated with canal diameter (R=-0.45, Fig. 4.6). While the correlations with size are expected, the strength of the correlation with thickness near the articular surface and the lack of a stronger correlation with diameter are notable. The latter is a significant consideration in implant design, supporting the need for modularity including varying head offsets to reproduce head center independent of stem diameter.

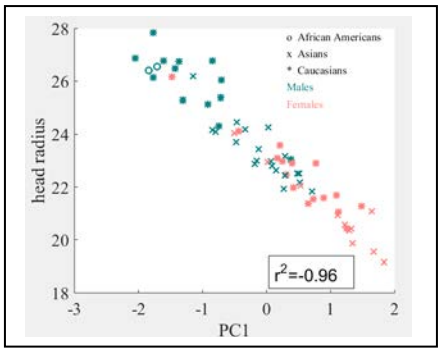

Figure 4.3: Mode 1 vs. head radius.

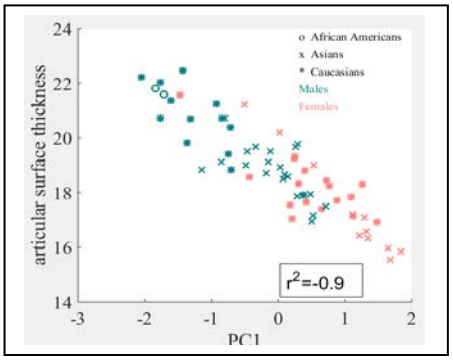

Figure 4.4: Mode 1 vs. articular surface thickness.

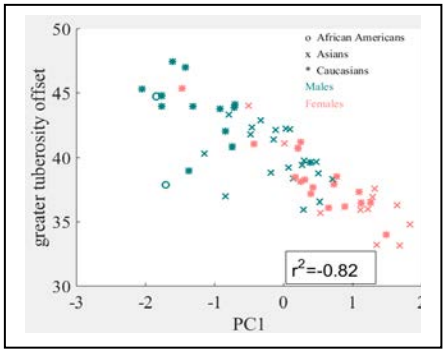

Figure 4.5: Mode 1 vs. greater tuberosity offset.

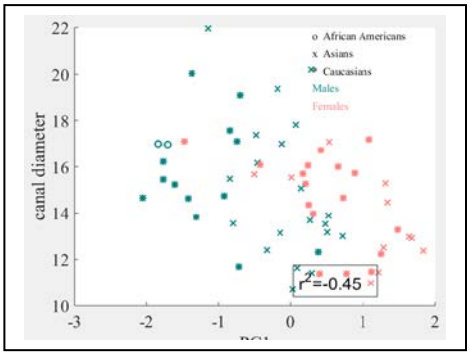

Figure 4.6: Mode 1 vs. canal diameter.

Mode 2 did not result in a correlation with any of the anatomic measurements assessed where R was greater than or equal to 0.30. This is because mode 2 captured changes near the lesser tuberosity (Fig. 4.2) and common clinical and anatomical measurements do not typically consider this area. Mode 3 was strongly correlated with inclination (R=-0.94, Fig. 4.7), neck angle (R=0.88, Fig. 4.8), and medial offset (R=0.74, Fig. 4.9).

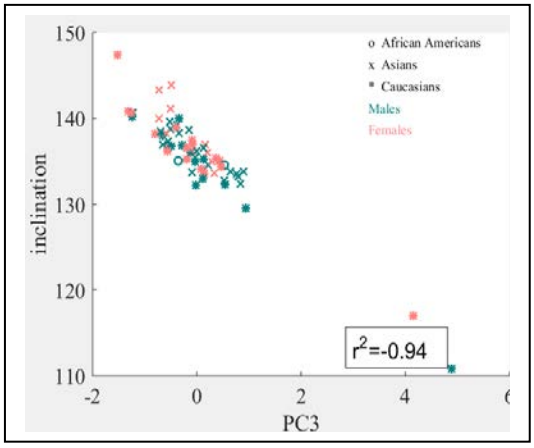

Figure 4.7: Mode 3 vs. inclination.

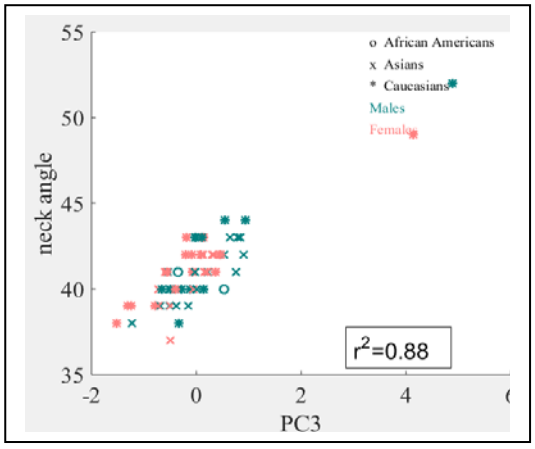

Figure 4.8: Mode 3 vs. neck angle.

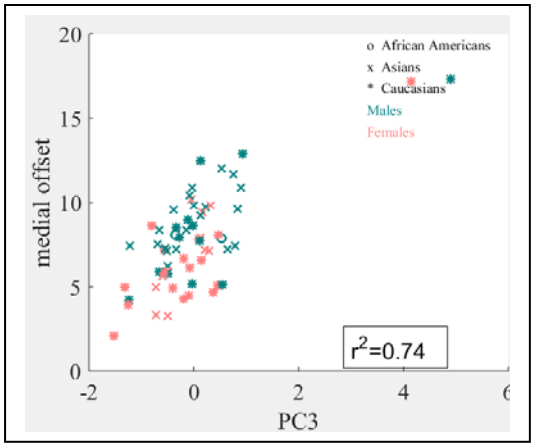

Figure 4.9: Mode 3 vs. medial offset.

Mode 4 was moderately correlated with canal diameter (R=0.59, Fig. 4.10), and weakly correlated with AP offset (R=-0.32, Fig. 4.11).

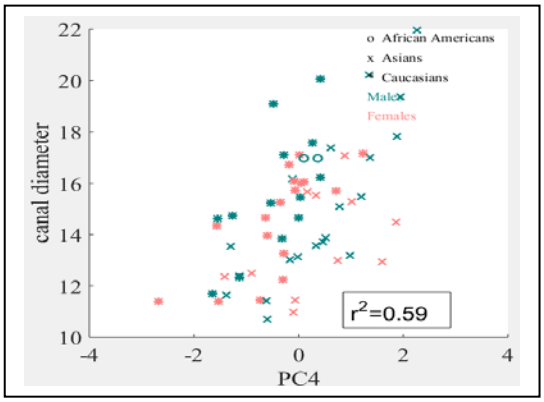

Figure 4.10: Mode 4 vs. canal diameter.

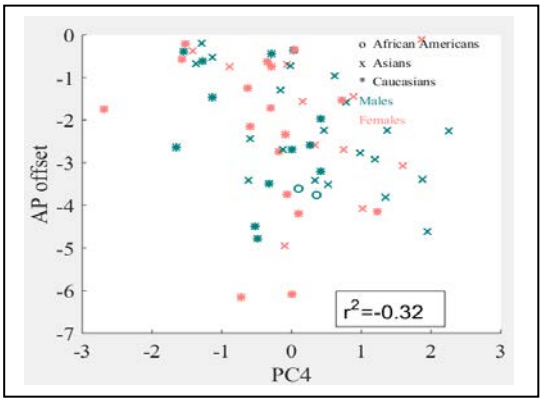

Figure 4.11: Mode 4 vs. AP offset.

4.4 Anatomical Measurement Correlations

All anatomical measurements were analyzed for correlation when compared to each other, with consideration given when R was greater than or equal to 0.30 (Table 4.1).

Table 4.1: Anatomical measurement correlations.

All Subjects	head radius	neck angle	greater tuberosity offset	medial offset	AP offset	articular surface thickness	canal diameter	inclination	sphericity
head radius	1	X	**0.83**	X	X	**0.86**	**0.43**	X	X
neck angle		1	X	**0.56**	X	X	X	**0.94**	X
greater tuberosity offset			1	X	X	**0.83**	X	X	X
medial offset				1	**0.3**	X	X	**-0.76**	X
AP offset					1	X	X	**0.31**	X
articular surface thickness						1	X	X	X
canal diameter							1	X	X
inclination								1	X
sphericity									1

Correlation	strong	moderate	weak	X <0.30

When looking at correlations between anatomic measurements, head radius was strongly correlated with articular surface thickness (R=0.86, Fig. 4.12), and greater tuberosity offset (R=0.83, Fig. 4.13), and weakly correlated with canal diameter (R=0.43, Fig. 4.14).

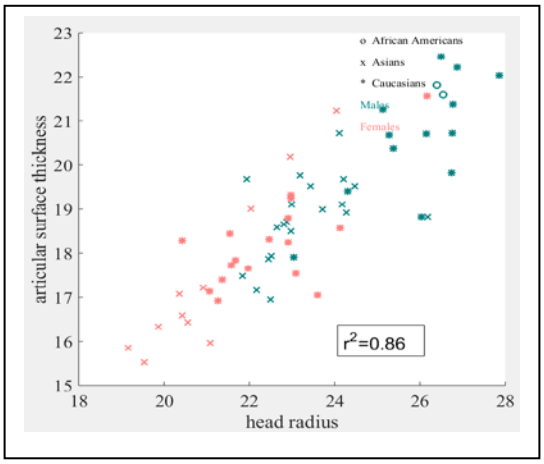

Figure 4.12: head radius vs. articular surface thickness.

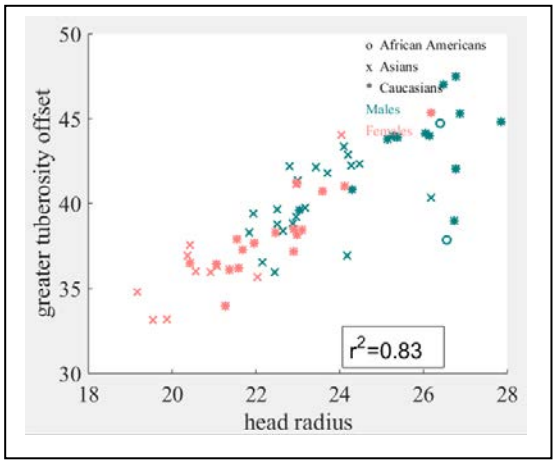

Figure 4.13: head radius vs. greater tuberosity offset.

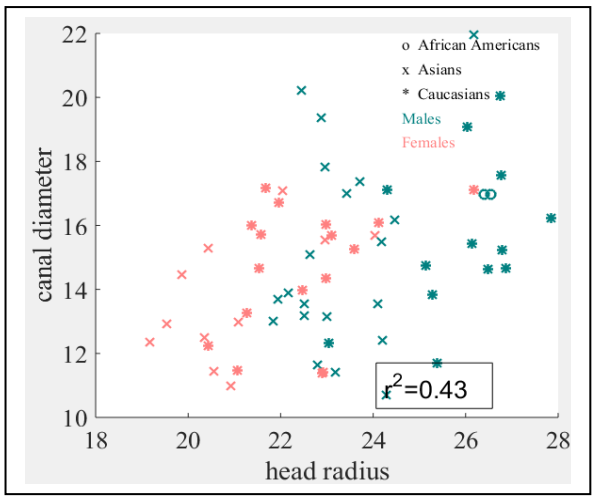

Figure 4.14: head radius vs. canal diameter.

As expected, neck angle was strongly correlated with inclination (R=0.94, Fig. 4.15), as the anatomic neck angle is relational to the head inclination angle. It was also moderately correlated with medial offset (R=0.56, Fig. 4.16).

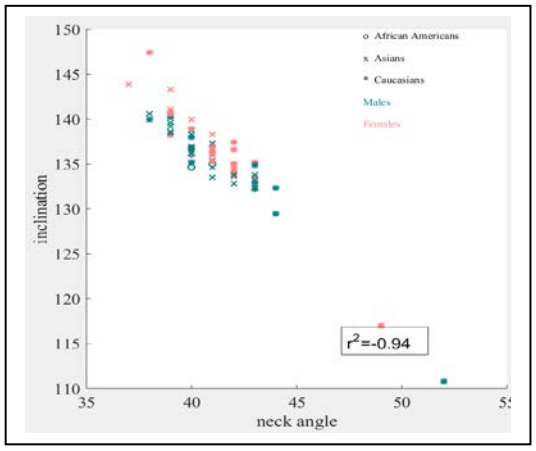

Figure 4.15: neck angle vs. inclination.

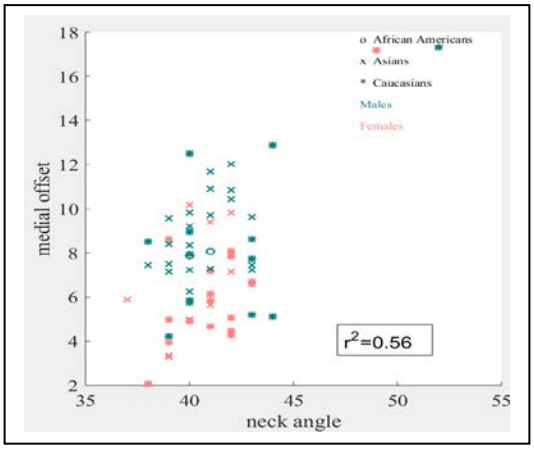

Figure 4.16: neck angle vs. medial offset.

Greater tuberosity offset was strongly correlated with articular surface thickness (R=0.83, Fig. 4.17), and there was a weak correlation between AP offset and inclination (R=0.31, Fig. 4.18).

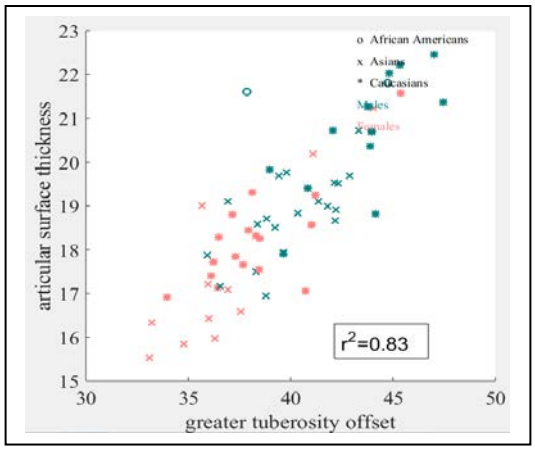

Figure 4.17: greater tuberosity offset vs. articular surface thickness.

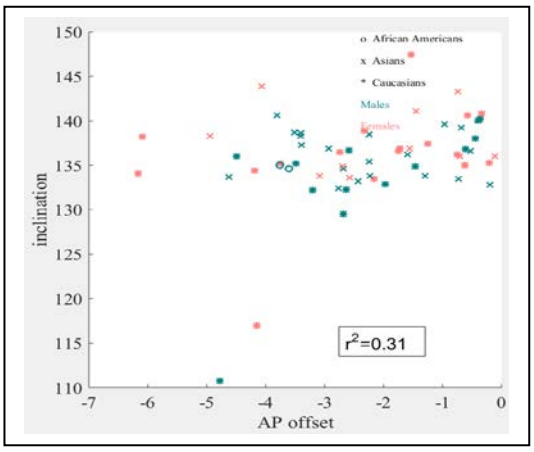

Figure 4.18: AP offset vs. inclination.

Finally, medial offset was strongly correlated with inclination (R=-0.76, Fig. 4.19) and weakly correlated with AP offset (R=-0.30, Fig. 4.20).

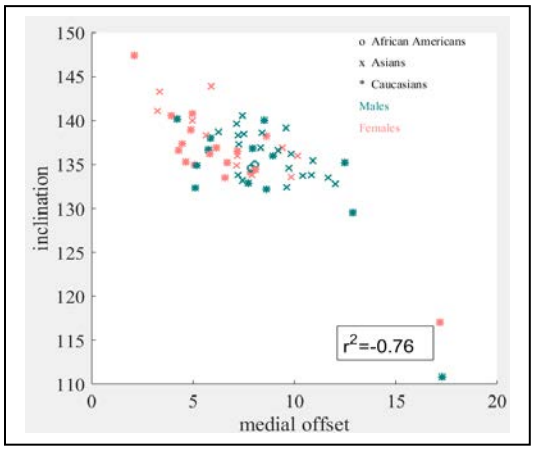

Figure 4.19: medial offset vs. inclination.

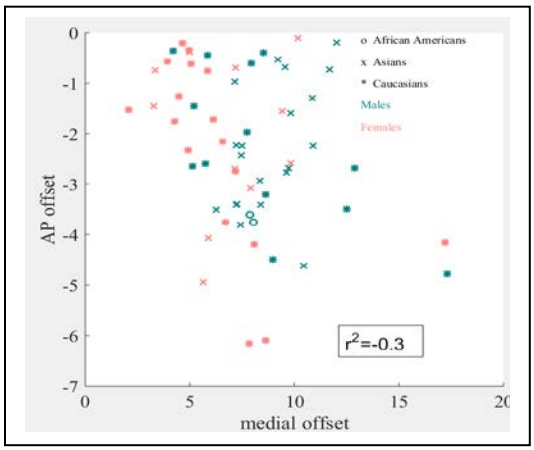

Figure 4.20: medial offset vs. AP offset.

Many of these anatomical measurement correlations can be attributed to the normal scaling or size change of the bone that was captured in mode 1 (Fig. 4.2) such as head radius versus greater tuberosity offset, articular surface thickness, or canal diameter, as well as greater tuberosity offset versus articular surface thickness. As previously mentioned neck angle and inclination are complimentary measurements so this correlation would be expected.

Other measurements were not inherently expected and drove further investigation. These included: medial offset versus inclination, medial offset versus neck angle, AP offset versus inclination, and medial offset versus AP offset. These correlations were analyzed at

the subpopulation level to determine if a specific ethnicity or gender were driving the relationship.

Medial offset versus inclination showed a strong correlation of R=-0.76 (Fig. 4.19). When looking at subpopulations for this group, the correlations remained relatively consistent, with Caucasian females having a slightly higher correlation (R=-0.90) than the other subgroups (Table 4.2).

Table 4.2: Subgroup correlations for medial offset vs. inclination.

medial offset vs. inclination									
Population	**All**	**Caucasians**	**Asians**	**Males**	**Females**	**Caucasian Females**	**Asian Females**	**Caucasian Males**	**Asian Males**
R value	-0.76	-0.84	-0.72	-0.69	-0.84	-0.90	-0.77	-0.77	-0.61
# Subjects	63	30	31	35	28	17	11	13	20

The relationship between medial offset and neck angle (R=0.56, Fig. 4.16) showed similar results with Caucasian females having the highest correlation (R=0.81, Table 4.3). This similarity was to be expected since medial offset was being compared to complimentary measurements (inclination and neck angle) in these two analyses.

Table 4.3: Subgroup correlations for medial offset vs. neck angle.

medial offset vs. neck angle									
Population	**All**	**Caucasians**	**Asians**	**Males**	**Females**	**Caucasian Females**	**Asian Females**	**Caucasian Males**	**Asian Males**
R value	0.56	0.7	0.41	0.52	0.7	0.81	0.54	0.63	0.33
# Subjects	63	30	31	35	28	17	11	13	20

AP offset versus inclination showed varying results among the subgroups with several having no correlation (Table 4.4). The weak correlation for the entire subject pool (R=0.31, Fig. 4.18) was likely driven by the moderate correlation for Caucasian males (Fig. 4.21), which in turn was driven by ethnicity and/or gender, as Caucasians showed a weak correlation while Asians showed none, and males showed a weak correlation and females did not.

Table 4.4: Subgroup correlations for AP offset vs. inclination.

AP offset vs. inclination									
Population	**All**	**Caucasians**	**Asians**	**Males**	**Females**	**Caucasian Females**	**Asian Females**	**Caucasian Males**	**Asian Males**
R value	0.31	0.46	<0.3	0.35	<0.3	0.35	<0.3	0.66	<0.3
# Subjects	63	30	31	35	28	17	11	13	20

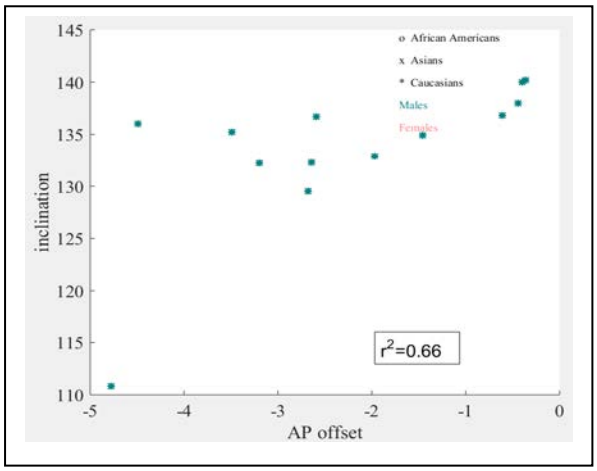

Figure 4.21: AP offset vs. inclination.

Medial offset was weakly correlated (R = 0.3) with AP offset for the entire subject population (Fig. 4.20). While AP offset is defined as the distance from the axis of the medullary canal to the center of the humeral head in the anterior-posterior direction, no

subjects exhibited anterior offset. AP offset ranged from 0.11 to 6.16 mm in the posterior direction only. Subpopulations showed varying results for the medial offset versus AP offset correlation with three subgroups exhibiting a moderate correlation, two showing a weak correlation, and three with no correlation (Table 4.5).

Table 4.5: Subgroup correlations for medial offset vs. AP offset.

medial offset vs. AP offset									
Population	**All**	**Caucasians**	**Asians**	**Males**	**Females**	**Caucasian Females**	**Asian Females**	**Caucasian Males**	**Asian Males**
R value	-0.3	-0.57	<0.3	<0.3	-0.41	-0.59	<0.3	-0.65	0.46
# Subjects	63	30	31	35	28	17	11	13	20

The weak correlation for all subjects was driven by a moderate correlation in the Caucasian population (R=0.57, Fig. 4.22). There was no correlation in the full Asian population ((R<0.30, Fig. 4.23).

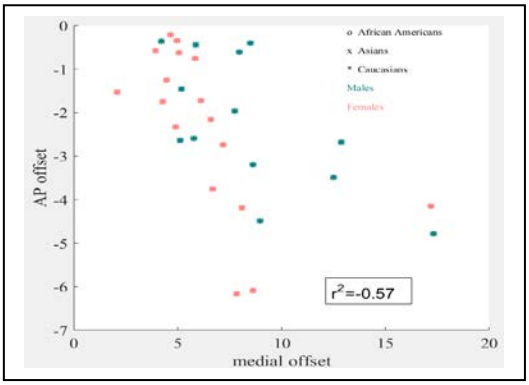

Figure 4.22: medial offset vs. AP offset – Caucasians.

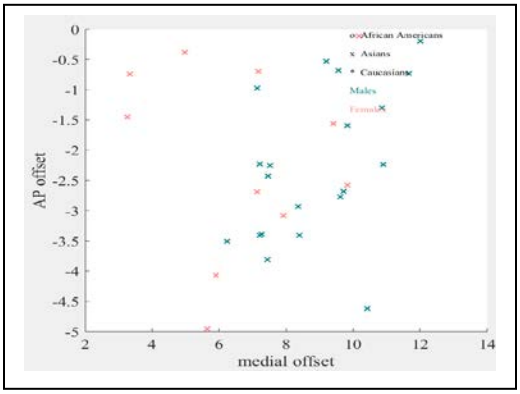

Figure 4.23: medial offset vs. AP offset – Asians.

There was no correlation for males for medial offset versus AP offset when looking at the entire male population (R<0.30, Fig. 4.24). For females there was a weak correlation (R=-0.41, Fig. 4.25).

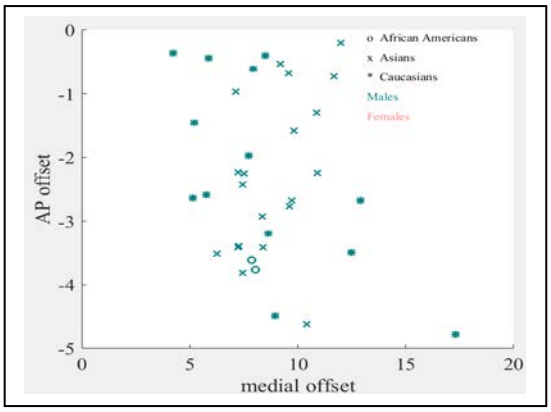

Figure 4.24: medial offset vs. AP offset – males.

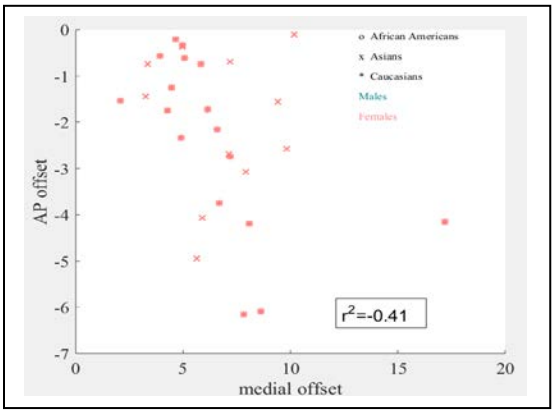

Figure 4.25: medial offset vs. AP offset – females.

Caucasian females had a moderate correlation between medial and posterior offsets (R=-0.59, Fig. 4.26). Asian females did not have a correlation (R<0.30, Fig. 4.27). As medial offset increased, so did posterior offset for Caucasian females.

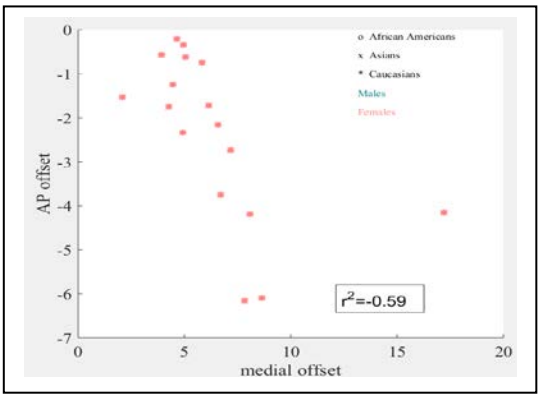

Figure 4.26: medial offset vs. AP offset – Caucasian females.

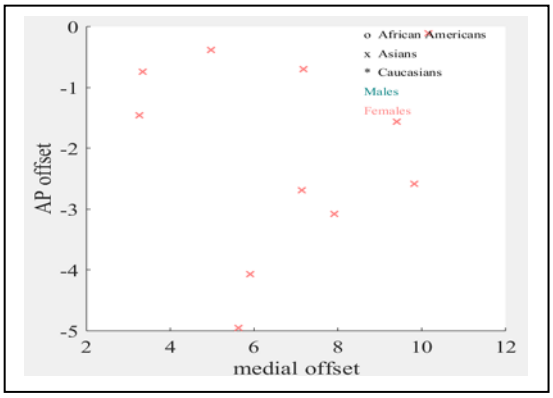

Figure 4.27: medial offset vs. AP offset – Asian females.

Caucasian males exhibited a moderate correlation between medial and AP offsets (R=-0.65, Fig. 4.28). Asian males had a weaker correlation (R=0.46) than Caucasian males.

For Caucasian males, as medial offset increased, so did posterior offset. However, the opposite was true for Asian males: as the medial offset increased, the posterior offset decreased (Fig. 4.29).

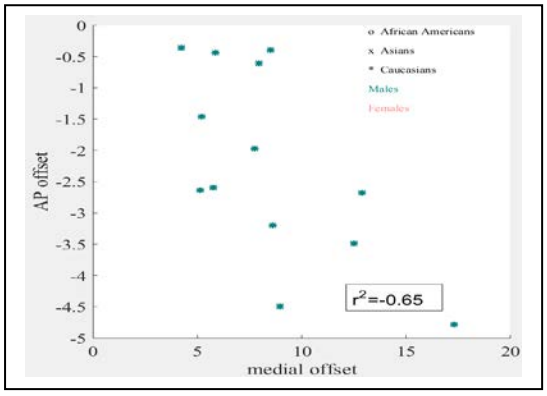

Figure 4.28: medial offset vs. AP offset – Caucasian males.

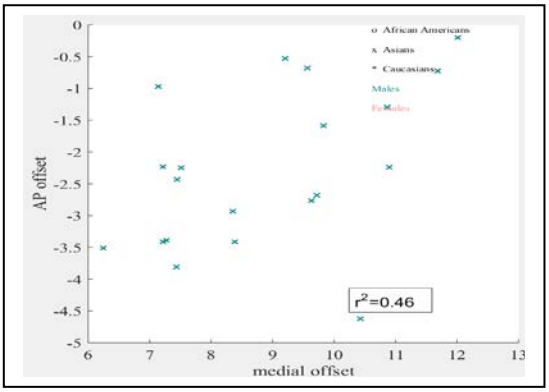

Figure 4.29: medial offset vs. AP offset – Asian males.

CHAPTER 5: DISCUSSION

A statistical shape model was developed and used to quantify variation in the cortical and cancellous bone or the proximal humerus for 63 subjects. Anatomical measurements were made related to regions of the humeral head and intramedullary canal and their relationships were analyzed. This chapter will discuss the results and their importance, limitations of this study, and potential future work.

5.1 Significance

The LOO analysis resulted in a root mean squared (RMS) error averaged across all nodes and all subjects of 0.89 mm with a standard deviation of 0.34 mm. This error assessed the statistical model's ability to describe variability in the training set and was small compared to prior studies (Table 5.1), suggesting that SSM methodology and execution continue to be refined.

Table 5.1: RMS error results for SSM studies.

Study	Year	RMS
this study	2017	0.89
Rao et al.	2013	1.64
Fitzpatrick et al.	2011	2.5 and below
Yang et al.	2008	1.39 and above

For both this study and Kamer et al. (2016), the majority of the variability in the training set, or PC1, was described by scaling of the bone. However, changes near the lesser tubercle were described by PC2 for this study, while the Kamer study reported variation in head inclination and the shaft. For this study, the first two principal components accounted for 85% of the variation: PC1 explained 75% of variation, and PC2 explained 10% of the variation. For the Kamer study, these first two principal components accounted for 65% of the variation.

Scaling accounted for 75% of the variation in the training set. Differences between males and females were primarily in size. While most shoulder implants are offered in a range of sizes to accommodate a range of patients, other changes in anatomy that could be important are often not accommodated for in implant design. For example, Mode 3 described changes in the medial curve of the neck (Fig. 5.1) and many implant designs

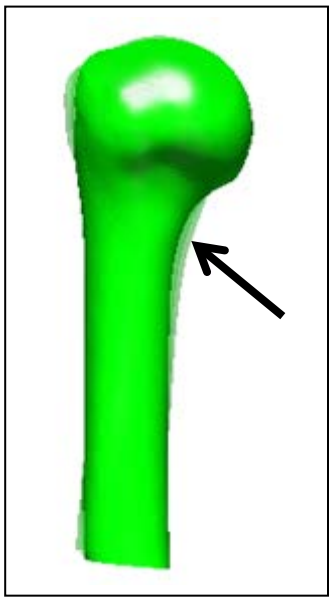

Figure 5.1: Mode 3 captured changes in medial curve.

offer a constant radius of curvature in this area regardless of the implant size. Fit of implant to bone is especially important along the medial curve during fracture surgery when this area of medial calcar is often the only solid bone left by which to align the implant.

Differences in ethnicity and/or gender were observed in the relationship between posterior offset and the head inclination angle. There was a moderate correlation for Caucasian males showing that as the head inclination angle increases, the posterior offset decreases. This was not evident for Asian males or Asian females, and there was only a weak correlation for Caucasian females.

Ethnicity differences were observed in the relationship between medial and posterior offset, with Caucasians showing a moderate correlation while Asians did not. More specifically, Caucasian males showed a moderate to strong correlation while Asian males showed a moderate negative correlation. Or, as the medial offset grew by 1mm, the posterior offset became larger in Caucasian males by 0.26 mm, but smaller in Asian males by 0.34mm.

Looking only at medial offset and AP offset for the entire population would show that to recreate the anatomic head center and utilize the intramedullary canal for stability, the implant design would need to be able to accommodate offsets ranging from 0 to 6mm posteriorly and 2 to 17mm medially. Figure 5.2 shows that a standard set of six humeral stem implants, used with a set of 4mm offset eccentric heads will cover offsets ranging from 4mm anterior to 4mm posterior, and from 1.1 to 14.7mm medially. This suggests that

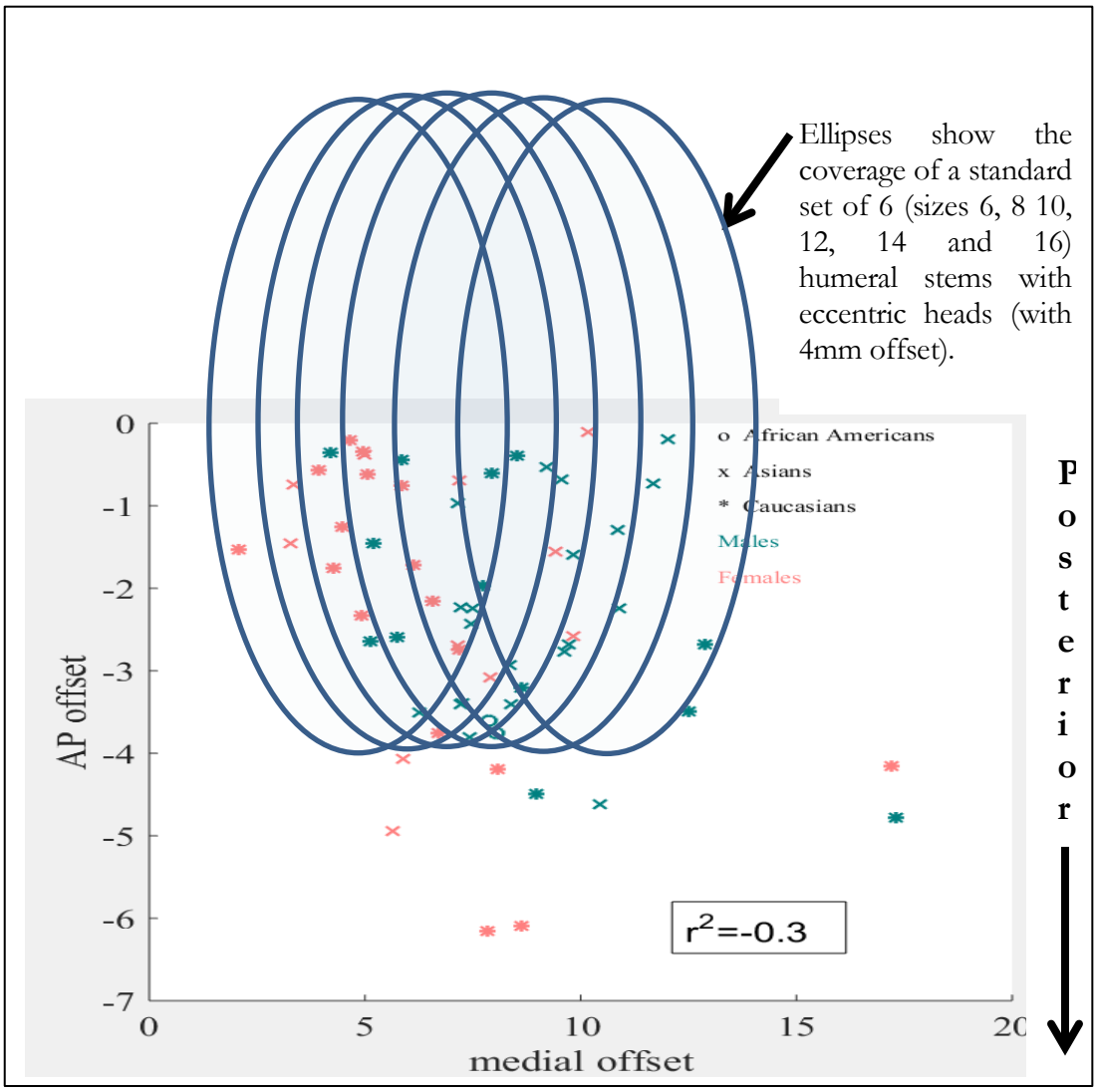

Figure 5.2: Medial offset vs. AP offset with implant offset ranges.

much of the population would be covered for these offsets, except for higher medial and posterior offsets. To recreate the head center of the highest offset patients with these implants the stem would need to rotated in canal. Based on this data, implant designs could incorporate a modest posterior offset in the stem and/or greater offset (eccentricity) in the head to better replicate anatomic offsets in a greater number of patients while maintaining

the original axis of the canal. However, a posterior offset stem would create left and right side stems, thereby doubling the needed stem inventory. Also, increasing the eccentricity of the humeral head would increase the moment arm being applied to the feature that connects with the stem, and this would need to be tested accordingly.

Within the training set, it should be noted that several outliers were present. Subjects with extremely high medial offsets (approximately 17mm, Figure 5.2) exhibited rotated (varus) humeral heads. Additionally, it has been shown that to replicate anatomic head center, medial osteophytes should be removed (Boileau and Walch, 1997; 1999). Therefore, offsets could actually be smaller if osteophytes were present.

5.2 Limitations

The entire humeral bone was not included in the scans for all 63 subjects. Therefore only the proximal portion of the humerus was included in the SSM. For consistency, the shaft of the humerus was resected at length relational to the head size. While this constrained the length of the bone to the size of the humeral head, it did not allow for alignment or geometry selection based off of the distal geometry of the humerus. Since retroversion is constructed off of the transepicondylar axis, it was not able to be calculated.

The anatomical coordinate system and anatomical measurements were based off of manually selected points. Measurements were done by manually selecting spots on anatomical landmarks and then placed on the template geometries. Based on corresponding node numbers, these were then automatically placed on each registered subject.

While the current training set of 63 subjects is larger than prior SSM studies of the shoulder (Kamer, 2016; Mustvanga, 2015; Drew, 2014), the majority (61) of the subject population was comprised of Asian and Caucasian subjects. Only 2 African-American subjects were in the study and the study population was therefore not fully representative of the global population. Breaking the population down for further analysis based on ethnicity and gender led to subgroups as small as 11 subjects, thereby decreasing confidence in the accuracy of the correlation results. For correlations, the terms strong ($R>0.7$), moderate ($0.5<R<0.7$), and weak ($0.3<R<0.5$) were used to characterize the strength of the correlations but do not show the true delineations of the R values.

Future work could include 2 sample t-tests to determine if differences between the subgroups are statistically relevant. Further analysis of the relationships between anatomical measurements by subgroups could be done as well. Additionally, more subjects could be added and more ethnicities could be added, and/or the subjects could be replaced with full size bones for potentially improved anatomic alignment.

5.3 Conclusion

This study used a methodological approach for statistical shape modeling to quantify variation in geometry of the proximal humerus. Sixty-three subject bones were processed and the data sets described relative to a training data set. The variations were statistically analyzed.

Differences in relationships between anatomical measurements relevant to shoulder arthroplasty were observed with ethnicity, while gender differences were mainly captured within the size variation.

Better understanding of the ethnic and gender differences in the geometry of the proximal humerus could inform the design of future shoulder implants and surgical instruments. This in turn could drive better replication of the original anatomy for better load transfer, and joint stability and mechanics, thereby leading to faster recoveries and better patient outcomes.

REFERENCES

Agency for Healthcare Research and Quality. Joint Replacement to Become the Most Common Elective Surgery in the Next Decades. February 2016. Issue 503. https://www.ahrq.gov/news/newsletters/e-newsletter/503.html.

American Academy of Orthopaedic Surgeons. OthoInfo: Shoulder Joint Replacement." http://orthoinfo.aaos.org/topic.cfm?topic=A00094. Accessed April 10, 2017.

Australian Orthopaedic Association National Joint Replacement Regisitry. Annual Report. Adelaide: AOA; 2016. 254-319, 350-353.

Bailie DS, Llinas PJ, Ellenbecker TS. Cementless Humeral Resurfacing Arthroplasty in Active Patients Less Than Fifty-five Years of Age. The Journal of Bone and Joint Surgery-American Volume. 2008;90(1):110-117. doi:10.2106/jbjs.f.01552.

Barratt DC, Chan CS, Edwards PJ, et al. Instantiation and registration of statistical shape models of the femur and pelvis using 3D ultrasound imaging. Medical Image Analysis. 2008;12(3):358-374. doi:10.1016/j.media.2007.12.006.

Behiels G, Maes F, Vandermeulen D, Suetens P. Evaluation of image features and search strategies for segmentation of bone structures in radiographs using Active Shape Models. Medical Image Analysis. 2002;6(1):47-62. doi:10.1016/s1361-8415(01)00051-2.

Besl, P, McKay N. A Method for Registration of 3-D Shapes". IEEE Trans. on Pattern Analysis and Machine Intelligence. 2002. Los Alamitos, CA, USA: IEEE Computer Society. 14 (2): 239–256.

Boileau P, Walch G. The Surgical Anatomy and Osteotomy Technique for the Humeral Head. 1999. Shoulder Arthroplasty. Springer, Berlin, Heidelberg.

Boileau P, Walch G. The Three-Dimensional Geometry of the Proximal Humerus: Implications for Surgical Technique and Prosthetic Design. The Journal of Bone and Joint Surgery. 1997;79(5):857-865. doi:10.1302/0301-620x.79b5.7579.

Boileau P, Watkinson DJ, Hatzidakis AM, Balg F. Grammont reverse prosthesis: Design, rationale, and biomechanics. Journal of Shoulder and Elbow Surgery. 2005;14(1). doi:10.1016/j.jse.2004.10.006.

Bredbenner T, Nicolella D, Statistical Shape and Density Based Finite

Element Modeling of the Human Proximal Femur. 2008. *Transactions of the 33rd Annual Meeting of the Orthopaedic Research Society*, San Francisco, CA, 0305.

Bryan R, Mohan PS, Hopkins A, Galloway F, Taylor M, Nair PB. Statistical modelling of the whole human femur incorporating geometric and material properties. Medical Engineering & Physics. 2010;32(1):57-65. doi:10.1016/j.medengphy.2009.10.008.

Center for Disease Control and Prevention (CDC). Prevalence and Most Common Causes of Disability Among Adults. MMWR Weekly Report. 2009: 58: 421-426.

Chen Y, Medioni G. Object modelling by registration of multiple range images. Image and Vision Computing. 1992;10(3):145-155. doi:10.1016/0262-8856(92)90066-c.

Cootes T, Taylor C, Cooper D, Graham J. Active Shape Models-Their Training and Application. Computer Vision and Image Understanding. 1995;61(1):38-59. doi:10.1006/cviu.1995.1004.

DePuy Synthes 0612-76-510. Total Shoulder Replacement. 2015. DSUS/JRC/0715/0942 7M 0815.

DePuy Synthes 0612-79-510. Reverse Shoulder Replacement. 2015. DSUS/JRC/0215/0732 7M 03/15.

DePuy Synthes 0612-81-510. Options for treating shoulder pain. 2015. DSUS/JRC/0614/0221 (1) 5M 02/15.

DePuy Synthes Joint Reconstruction, a division of DOI 2014. Shoulder resurfacing. 2014. 0612-77-510 (Rev 1) 2M 03/14.

Devijver PA, Kittler J. Pattern recognition: a statistical approach. Englewood Cliffs, N.J.: Prentice-Hall; 1982.

Drew A, Cates J, Morris A, Bachus K, Statistical Shape Modeling of the Humerus for Rapid Endoprosthic Stem Design Iteration. 2014. Annual Meeting of the Orthopaedic Research Society. Poster No: 0963.

Fitzpatrick C, Shape Analysis of the Resection Surfaces of the Knee in Relation to Implant Design. 2007. Ph.D. dissertation. University College Dublin.

Fitzpatrick CK, Baldwin MA, Laz PJ, Fitzpatrick DP, Lerner AL, Rullkoetter PJ. Development of a statistical shape model of the patellofemoral joint for

investigating relationships between shape and function. Journal of Biomechanics. 2011;44(13):2446-2452. doi:10.1016/j.jbiomech.2011.06.025.

Geisser S. Predictive inference: an introduction. New York, NY : Chapman and Hall; 1993. ISBN 0-412-03471-9.

Grossman R, Seni G, Elder J, Agarwal N, Liu H. Ensemble Methods in Data Mining: Improving Accuracy Through Combining Predictions. 2010. Morgan & Claypool. doi:10.2200/S00240ED1V01Y200912DMK002.

Hasan SS, Leith JM, Campbell B, Kapil R, Smith KL, Matsen FA. Characteristics of unsatisfactory shoulder arthroplasties. Journal of Shoulder and Elbow Surgery. 2002;11(5):431-441. doi:10.1067/mse.2002.125806.

Hertel R, Knothe U, Ballmer FT. Geometry of the proximal humerus and implications for prosthetic design. Journal of Shoulder and Elbow Surgery. 2002;11(4):331-338. doi:10.1067/mse.2002.124429.

Humphrey CS, Sears BW, Curtin MJ. An anthropometric analysis to derive formulae for calculating the dimensions of anatomically shaped humeral heads. Journal of Shoulder and Elbow Surgery. 2016;25(9):1532-1541. doi:10.1016/j.jse.2016.01.032.

Johnson MH, Paxton ES, Green A. Shoulder arthroplasty options in young (<50 years old) patients: review of current concepts. Journal of Shoulder and Elbow Surgery. 2015;24(2):317-325. doi:10.1016/j.jse.2014.09.029.

Jolliffe I. Principal Component Analysis. 2002. 2nd ed. Springer Series in Statistics. New York: Springer-Verlag.

Kamer L, Noser H, Popp AW, Lenz M, Blauth M. Computational anatomy of the proximal humerus: An ex vivo high-resolution peripheral quantitative computed tomography study. 2016. Journal of Orthopaedic Translation, 4, 46-56.

Kohavi R. A study of cross-validation and bootstrap for accuracy estimation and model selection. 1995.Proceedings of the Fourteenth International Joint Conference on Artificial Intelligence. San Mateo, CA: Morgan Kaufmann. 2 (12): 1137–1143.

Krueger F. A vitollium replica arthroplasty on shoulder. A case report of aseptic necrosis of the proximal end of the humerus. Surgery 1951, 30 1004-l 1.

Laz PJ, and Browne M. A review of probabilistic analysis in orthopaedic biomechanics. 2009. Proc. IMechE Vol. 224 Part H: J. Engineering in Medicine,927-943. DOI: 10.1243/09544119JEIM739.

Levy O, Copeland SA. Cementless surface replacement arthroplasty of the shoulder. The Journal of Bone and Joint Surgery. 2001;83(2):213-221. doi:10.1302/0301-620x.83b2.11238.

Mcpherson EJ, Friedman RJ, An YH, Chokesi R, Dooley R. Anthropometric study of normal glenohumeral relationships. Journal of Shoulder and Elbow Surgery. 1997;6(2):105-112. doi:10.1016/s1058-2746(97)90030-6.

Meller S, Kalender W. Building a statistical shape model of the pelvis.2004. International Congress Series, 1268, 561-566.

Mutsvangwa T, Burdin V, Schwartz C, Roux C. An Automated Statistical Shape Model Developmental Pipeline: Application to the Human Scapula and Humerus. IEEE Transactions on Biomedical Engineering. 2015; 62:1098-1107

Myronenko A, Song X. Point Set Registration: Coherent Point Drift. IEEE Transactions on Pattern Analysis and Machine Intelligence. 2010;32(12):2262-2275. doi:10.1109/tpami.2010.46.

Rajamani KT, Styner MA, Talib H, Zheng G, Nolte LP, Ballester MAG. Statistical deformable bone models for robust 3D surface extrapolation from sparse data. Medical Image Analysis. 2007;11(2):99-109. doi:10.1016/j.media.2006.05.001.

Rao C, Fitzpatrick CK, Rullkoetter PJ, Maletsky LP, Kim RH, Laz PJ. A statistical finite element model of the knee accounting for shape and alignment variability. Medical Engineering & Physics. 2013;35(10):1450-1456. doi:10.1016/j.medengphy.2013.03.021.

Schlens J. A Tutorial on Principal Component Analysis: Derivation, Discussion and Singular Value Decomposition.2003. 25 March.

Shim V, Pitto R, Streicher R, Hunter P, Anderson I.Development and validation of patient-specific finite element models of the hemipelvis generated from a sparse CT data set. 2008. Journal of Biomechanical Engineering - Transactions of the ASME, 130(5).

Yang YM, Rueckert D, Bull AMJ. Predicting the shapes of bones at a joint: application to the shoulder. Computer Methods in Biomechanics and Biomedical Engineering. 2008;11(1):19-30. doi:10.1080/10255840701552721.

Zhang Z. Iterative point matching for registration of free-form curves and surfaces. International Journal of Computer Vision. 1994;13(2):119-152. doi:10.1007/bf01427149.

Zheng G, Gollmer S, Schumann S, Dong X, Feilkas T, Ballester MAG. A 2D/3D correspondence building method for reconstruction of a patient-specific 3D bone surface model using point distribution models and calibrated X-ray images. Medical Image Analysis. 2009;13(6):883-899. doi:10.1016/j.media.2008.12.003.

APPENDIX A – TRAINING SET TABLE

Subject	Age	Sex	Ethnic group/race	Height (in)	Weight (lbs)	BMI	R/L	Humerus Length	Cortical Head Radius
S0 (Template)	82	M	Caucasian	68	185	28	L	Partial	24.4
S1	96	F	Caucasian	63	127	22	R	Partial	20.8774
S2	84	M	Caucasian	72	113	15	L	Partial	26.7349
S3	73	F	Thailand				R	Full	17.779
S4	96	F	Caucasian	63	127	22	R	Partial	21.5719
S5	56	M	Caucasian	75	126	16	R	Full	17.779
S6	69	F	Caucasian	66	126	20.33	L	Partial	24.1237
S7	73	M	Caucasian	67	119	18.64	L	Full	24.1903
S8	86	F	Caucasian	65	145		L	Full	19.4944
S9	87	F	Caucasian	63	110	19.48	R	Full	21.1596
S10	89	M	Caucasian	69	138	20.38	R	Full	25.3624
S11	78	F	Caucasian	60	130	25.39	L	Full	20.7231
S12	77	M	Caucasian	77	145	22.04	R	Full	23.7834
S13	89	F	Caucasian	64	160	27.46	L	Full	22.0715
S14	73	M	Japan				L	Full	22.3853
S15	69	M	Japan				L	Full	24.2924
S16	89	F	Japan				L	Full	19.6347
S17	78	M	Japan				L	Full	21.7023
S18	62	M	Japan				L	Full	20.949
S19	57	F	Japan				L	Full	19.6295
S20	50	M	Japan				L	Full	22.5073
S21	92	M	Japan				L	Full	21.4165
S22	88	M	Japan				L	Full	21.4553
S23	70	F	Japan				L	Full	18.14
S24	66	M	Japan				L	Full	21.7804
S25	83	M	Japan				L	Full	21.1529
S26	79	F	Japan				L	Full	22.7163
S27	86	F	Japan				L	Full	19.5443
S28	69	M	Japan				L	Full	20.4339
S29	85	M	Japan				L	Full	22.7341
S30	69	M	Japan				R	Full	23.2621
S31	30	F	Japan				L	Full	19.6058
S32	86	F	Japan				L	Full	19.1226
S33	73	F	Japan				L	Full	21.7811
S34	72	F	Caucasian	63	188	33.3	L	Full	21.1192
S35	80	M	Thailand				R	Full	24.5321

S36	60	M	Thailand				R	Full	22.7315
S37	68	F	Thailand				R	Full	21.8801
S38	44	M	Thailand				R	Full	21.943
S39	85	M	Thailand				R	Full	22.3352
S40	64	M	Thailand				R	Full	22.5743
S41	60	F	Thailand				R	Full	19.8733
S42	92	F	Caucasian	61	138	26	L	Partial	19.98
S43	60	M	Thailand				R	Full	20.5203
S44	60	M	Thailand				R	Full	22.8775
S45	66	M	Thailand				R	Full	20.5
S46	78	F	Caucasian	61	150	28.34	L	Full	19.805
S47	87	M	Caucasian	70	190	27.26	L	Full	25.5609
S48	59	M	Caucasian	74	134	17.2	L	Full	23.4611
S49	90	M	Caucasian	62	135	24.69	L	Full	24.523
S50	70	F	Caucasian	64	150	25.74	R	Full	20.749
S51	68	F	Caucasian	62	110	20.12	L	Full	21.8528
S52	83	M	Caucasian	65	140	23.29	L	Full	20.9881
S53	87	F	Caucasian	65	90	14.98	L	Partial	20.0162
S54	51	M	Caucasian	71	250	34.86	R	Partial	22.7637
S55	89	M	Caucasian	68	150	22.8	R	Partial	24.9776
S56	73	M	African American	74	150	19.26	L	Partial	24.4964
S57	75	F	Caucasian	67	100	15.66	L	Partial	20.6464
S58	73	F	Caucasian	60	70	13.67	R	Partial	19.5063
S59	79	F	Caucasian	67	120	18.79	L	Partial	22.4908
S60	73	M	African American	74	150	19.26	L	Partial	24.1237
S61	67	F	Caucasian	67	100	15.66	L	Partial	25.532
S62	86	M	Caucasian	69	185	27.32	R	Full	24.2196
S63	90	F	Caucasian	66	72	11.62	L	Full	21.0328

APPENDIX B – DEFINITIONS OF ANATOMICAL MEASUREMENTS

Definitions of Anatomical Measurements for Proximal Humerus

Developed by: Irene Sintini

Anatomical coordinate systems

Each bone was represented in the template anatomical coordinate system, defined similarly to [1]. For the humerus, the origin was placed in the glenohumeral rotational center, estimated as the center of the best-fitting sphere for the humeral head; the mediolateral axis was defined by the direction of the segment connecting the two epicondyles, pointing medially; the anterior-posterior axis was defined as the perpendicular to the plane of the glenohumeral rotational center and the epicondyles, pointing anteriorly; the superior-inferior axis was defined consequently to form a right-hand coordinate system (Fig. 1).

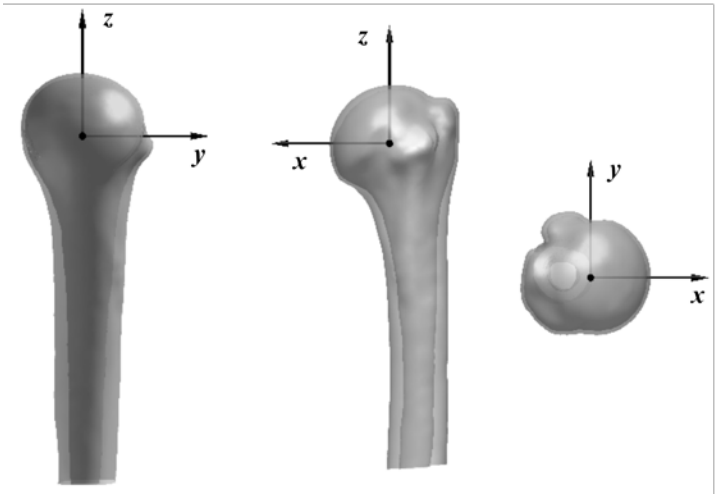

Figure 1. Humerus (above) and scapula (below) templates anatomical coordinate systems.

Anatomical landmarks

Anatomical landmarks were manually placed on the template geometries and then automatically selected on each registered subject, based on node numbers. They were used to automatically compute anatomical measurements on each registered subject and also to build the anatomical coordinate systems.

- **Humerus**
  1. Greater tuberosity (GT)
  2. Most anterior point of the anatomic neck (MA)
  3. Most posterior point of the anatomic neck (MP)
  4. Most lateral point of the anatomic neck (ML)
  5. Most medial point of the anatomic neck (MM)
  6. Superior apex of the head (SA)

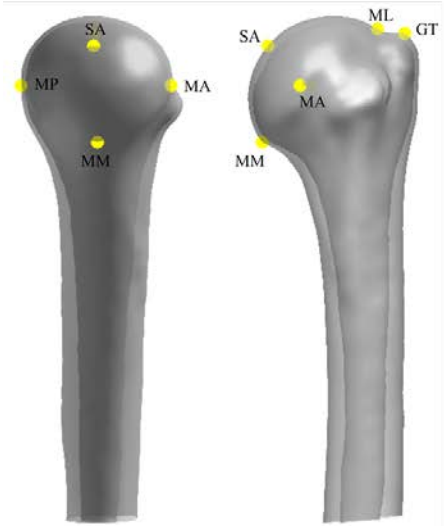

Figure 2. Humerus (left) anatomical landmarks.

Anatomical measurements

- **Humerus**

1. *Head radius*

   The head radius was computed as the radius of the sphere that best fits the humeral head (Figure 3), i.e. the epiphyseal sphere (Boileau and Walch, 1997). The nodes used to find the best-fitting sphere are selected manually on the cortical shell of the template and then used for all the subjects in the register.

2. *Canal diameter*

   The canal diameter was computed as the diameter of the cylinder that best fits the most inferior half of the cancellous shaft (Figure 3), i.e. the metaphyseal cylinder (Boileau and Walch, 1997). The axis of this cylinder is the canal axis (orthopaedic axis). This method gives an estimate that does not take into account how the canal diameter may vary along the shaft. If it is of interest to compute the diameter at specific sections of the shaft, this can be measured as the minimum distance between the most anterior and the most posterior point and the most medial and the most lateral point, or as the diameter of the best-fitting circle.

3. *Head sphericity*

   Head sphericity was computed as the ratio between the radii of the best-fitting circles in the X (mediolateral) - Z (superior-inferior) plane and Y (anterior-posterior) - Z (superior-inferior) plane (Figure 4). X-Z is the frontal plane; Y-Z is the sagittal plane. The points used to find the best-fitting circles come from the projections of the points used to find the best-fitting sphere on the fontal and sagittal plane; to make the code more robust, only the points above the origin are selected.

4. *Anatomical neck angle*

   The anatomic neck angle was computed as the angle that the vector connecting the most medial point of the anatomic neck and the most lateral point of the anatomic neck forms with the Z-axis (Figure 5).

5. *Greater tuberosity offset (or critical distance)*

   As defined in (Hertel et al., 2002), the greater tuberosity offset (or critical distance) is the distance between the most medial point of the anatomical neck and the canal axis in the X (mediolateral) - Z (superior-inferior) plane (Figure 5).

6. *Articular surface thickness*

   As defined in (Boileau and Walch, 1997), the articular surface thickness is the distance between the articular margin plane and the superior apex of the head, in the X (mediolateral) - Z (superior-inferior) plane (Figure 5).

7. *Inclination angle of the head*

   As defined in (Boileau and Walch, 1997), the inclination angle of the head is the angle between the canal axis and the perpendicular to the articular margin plane, in the X (mediolateral) - Z (superior-inferior) plane (Figure 5).

8. *Medial offset*

   As defined in (Boileau and Walch, 1997), the medial offset is the distance between the head center (i.e. the center of the best-fitting sphere) and the canal axis in the X (mediolateral) - Z (superior-inferior) plane (Figure 6).

9. *Anterior-posterior offset*

   As defined in (Boileau and Walch, 1997), the anterior-posterior offset is the distance between the head center (i.e. the center of the

best-fitting sphere) and the canal axis in the Y (anterior-posterior) - Z (superior-inferior) plane (Figure 6).

10. *Cortical thickness*

    The cortical thickness was computed as the distance between the cortical and the cancellous profile, at a specific section of the shaft, and at various angles (Figure 7). The distance was calculated both along the radial direction and along a direction normal to the cortical profile. An alternative, quicker method could be to calculate the difference between the diameter of the best-fitting cylinder in the cancellous bone and the best-fitting cylinder in the cortical bone. However, this method would not take into account how the thickness may vary with the superior-inferior and angular position.

Only the proximal portion of the humerus was included in the SSM. The humerus shaft was resected at the intersection with a sphere whose center was placed coincident with the head center and whose radius was proportional to the head radius (5.6 times). This constrained the length of the bone to the size of the humeral head. It was done because the entire bone was not available for all the 63 subjects. Given that the SSM was developed only on the proximal portion of the humerus, it was not possible to calculate the retroversion angle, since it is based on the transepicondylar axis. Only for the template, the center of the best-fitting sphere is actually the origin of the anatomical coordinate system. For all the other geometries, this is not exactly true. An alternative way to rigidly align the geometries would be to bring each one of them in its own anatomical coordinate system: in this way, the origin would always be the actual head center.

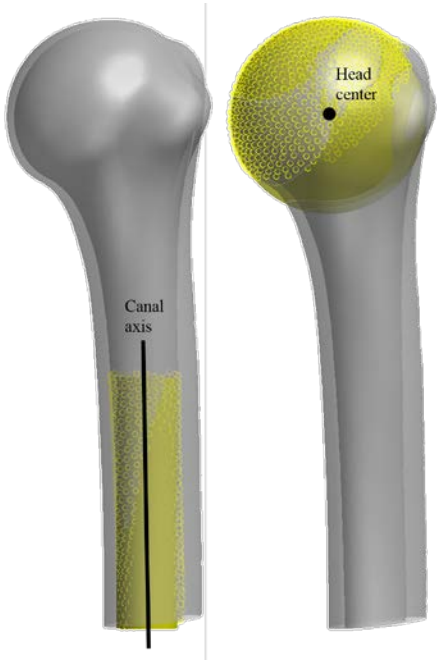

Figure 3. Best-fitting cylinder for the metaphyseal cylinder (left) and the best-fitting sphere for the humeral head (right). The nodes on the cortical shell used to find the bets-fitting geometries are represented as yellow scatter points; the analytical surfaces are represented in shaded yellow.

Figure 4. Best-fitting circles for the humeral head in the sagittal (left) and frontal (right) plane. The scatter points in yellow are the nodes used to find the bets-fitting circles (see Figure 3).

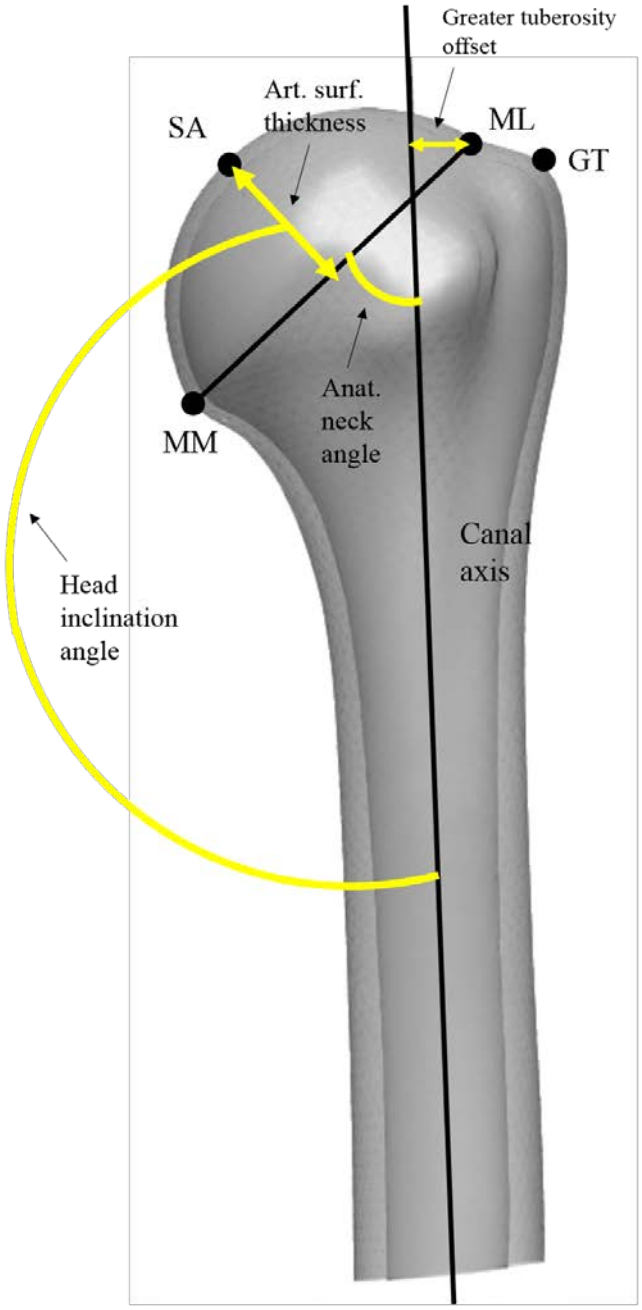

Figure 5. The humerus is represented in the X-Z plane to show the anatomical neck angle, the greater tuberosity offset or critical distance, the head inclination angle and the articular surface thickness.

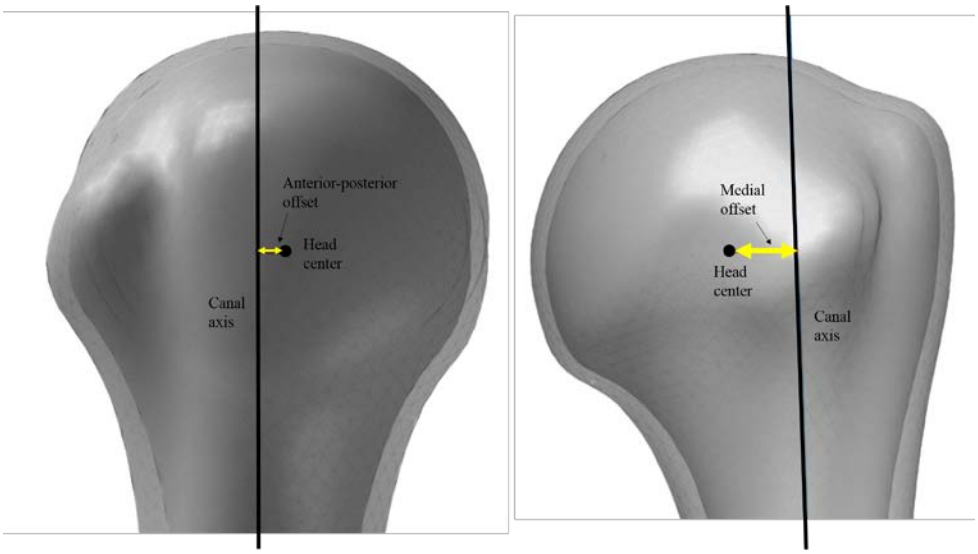

Figure 6. The humeral head is represented in the Y-Z plane (left) and the X-Z plane (right) to show respectively the anterior-posterior offset and the medial offset.

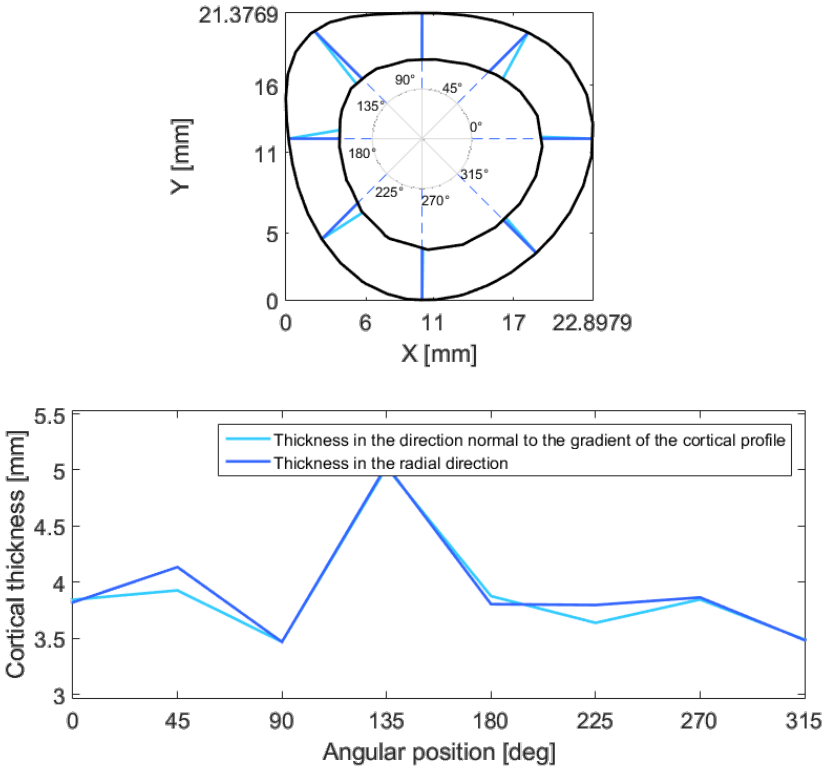

Figure 7. Cortical thickness was measured as the distance between cortical and cancellous profile at a specific section of the shaft (80 mm below the origin, for the case showed here), at various angles.